d-InSAR
-
Sub-cm Deformation Monitoring from Space

Franz J Meyer

Alaska Satellite Facility,
University of Alaska Fairbanks

Outline

- Theoretical Background of InSAR and d-InSAR
- Application of d-InSAR to various Geophysical Problems
- Limitations of d-InSAR
- An Introduction to Persistent Scatterer Interferometry (PSI)
- PSI Examples

Theoretical Background of InSAR and d-InSAR

SAR Interferometry ....

... combines two or more complex-valued SAR images to derive more information about the imaged objects (compared to using a single image) by exploiting phase differences.

$\Rightarrow$ Images must differ in at least one aspect (= “baseline”)

baseline type	**known as ...**	**applications: measurement of ...**
$\Delta\theta$	across-track	topography, DEMs
$\Delta t = \text{ms} \quad \text{to} \quad \text{s}$	along-track	ocean currents, moving object detection, MTI
$\Delta t = \text{days}$	differential	glacier/ice fields/lava flows, SWE, hydrology
$\Delta t = \text{days} \quad \text{to} \quad \text{years}$	differential	subsidence, seismic events volcanic activities, crustal displacements
$\Delta t = \text{ms} \quad \text{to} \quad \text{years}$	coherence estimator	sea surface decorrelation times land cover classification
$\Delta\nu_0$	Δk-radar	exact ranging, oceanography, SWE measurement

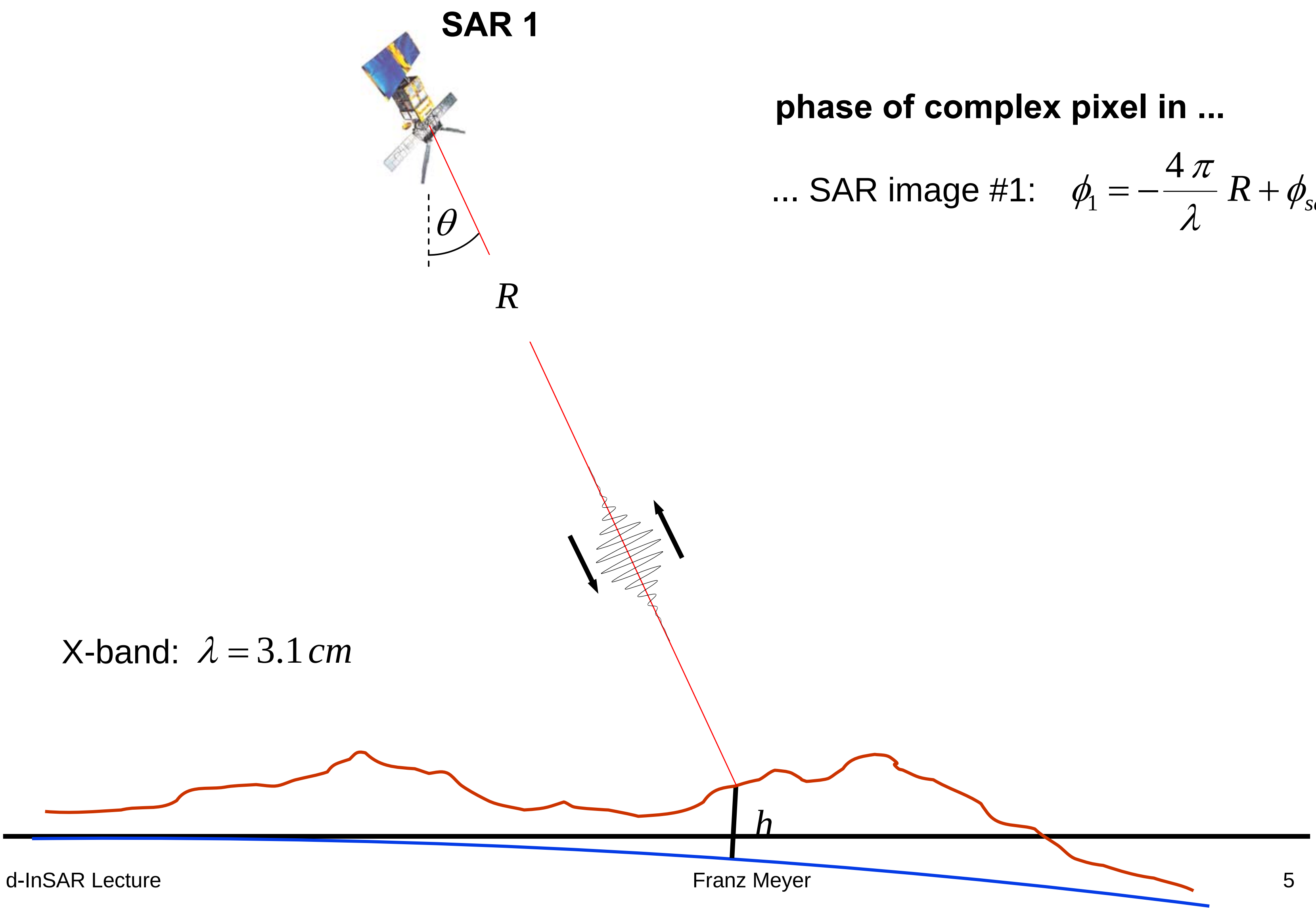

phase of complex pixel in ...

... SAR image #1: $\phi_1 = -\frac{4\pi}{\lambda} R + \phi_{scatt,1}$

X-band: $\lambda = 3.1\,cm$

Across-Track Interferometric Geometry

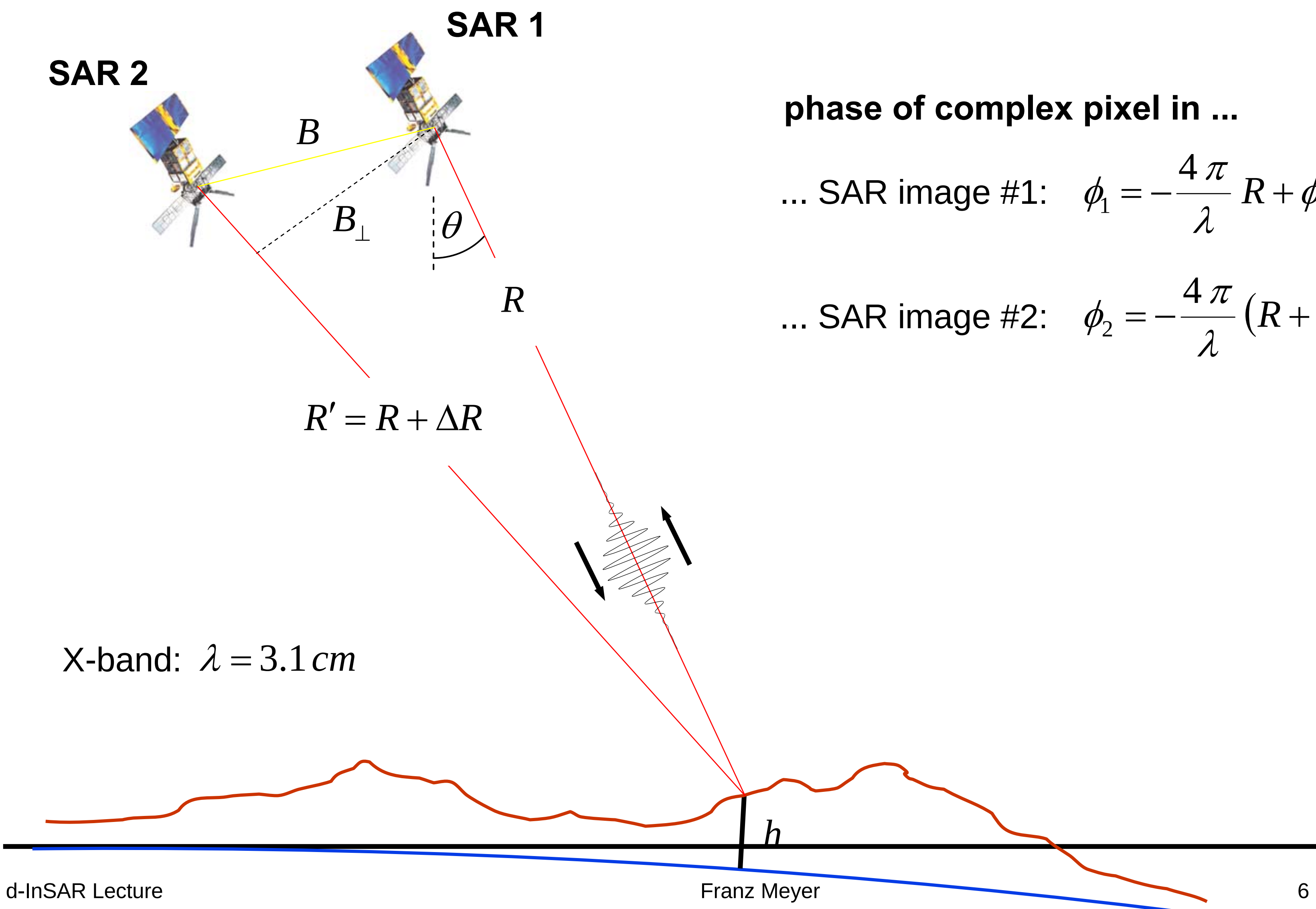

phase of complex pixel in ...

... SAR image #1: $\phi_1 = -\frac{4\pi}{\lambda} R + \phi_{scatt,1}$

... SAR image #2: $\phi_2 = -\frac{4\pi}{\lambda} (R + \Delta R) + \phi_{scatt,2}$

X-band: $\lambda = 3.1\, cm$

Across-Track Interferometric Geometry

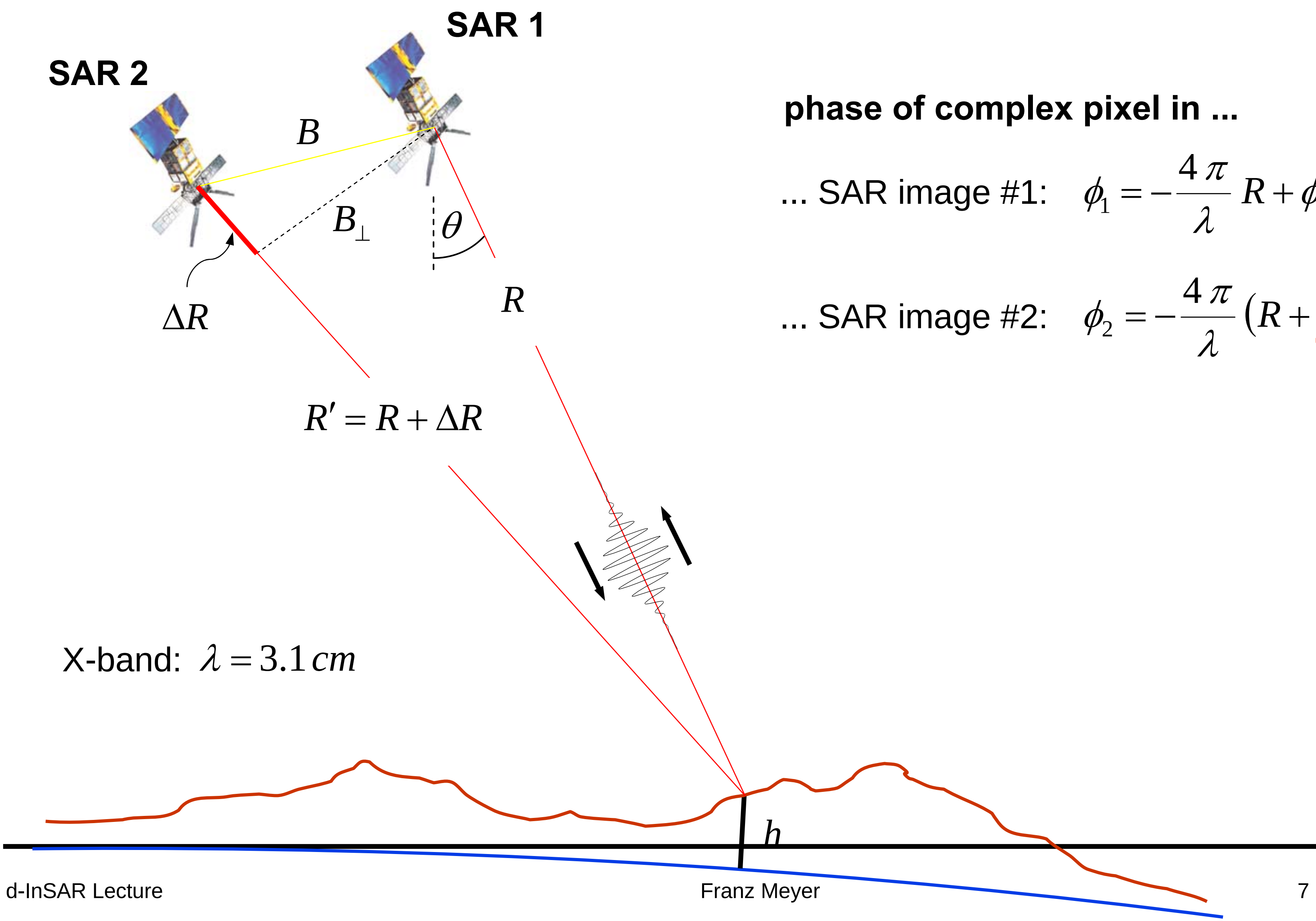

phase of complex pixel in ...

... SAR image #1: $\phi_1 = -\frac{4\pi}{\lambda} R + \phi_{scatt,1}$

... SAR image #2: $\phi_2 = -\frac{4\pi}{\lambda} (R + \underline{\Delta R}) + \phi_{scatt,2}$

X-band: $\lambda = 3.1\, cm$

Across-Track Interferometric Geometry

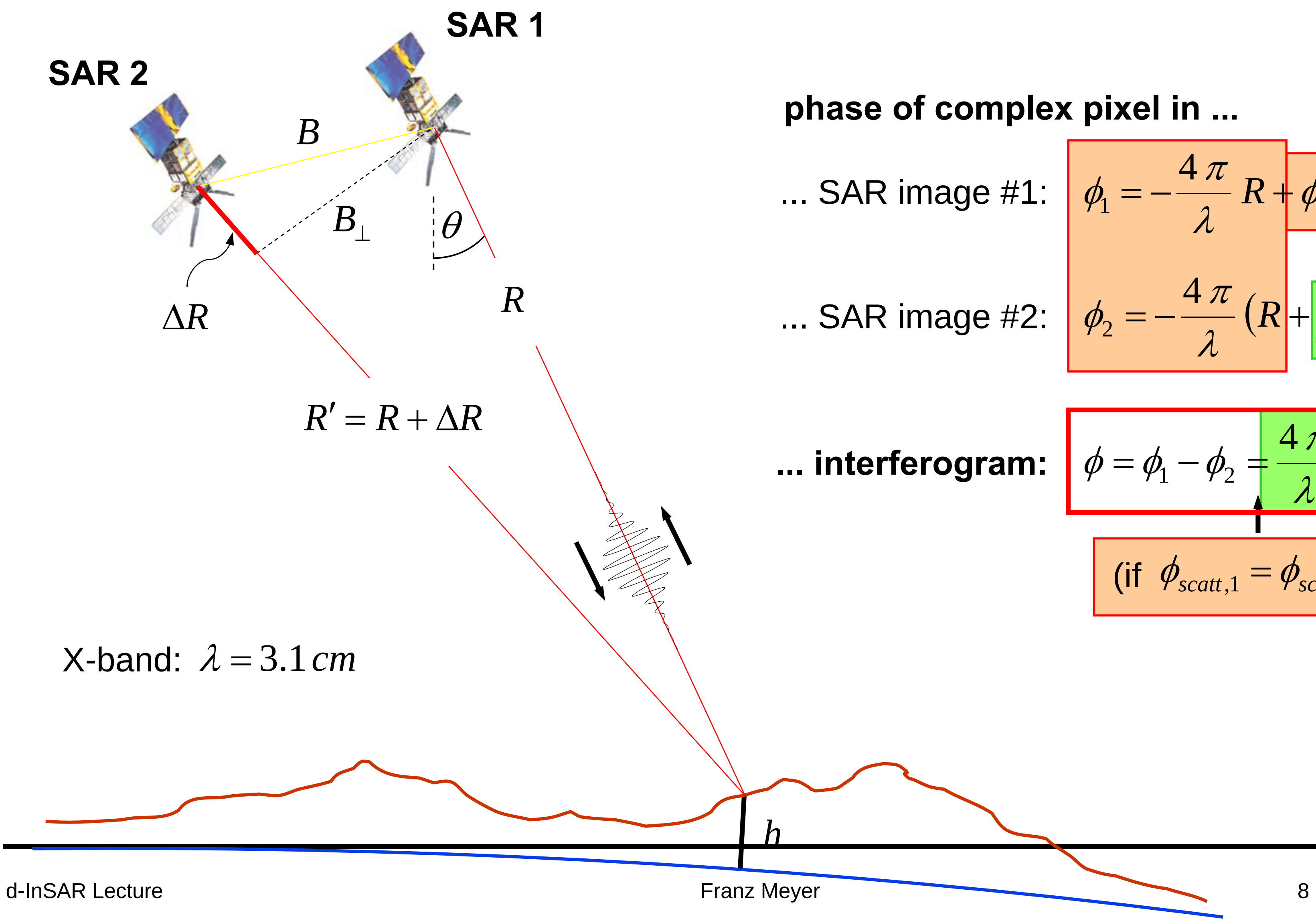

X-band: $\lambda = 3.1\,cm$

phase of complex pixel in ...

... SAR image #1: $\phi_1 = -\frac{4\pi}{\lambda} R + \phi_{scatt,1}$

... SAR image #2: $\phi_2 = -\frac{4\pi}{\lambda} (R + \Delta R) + \phi_{scatt,2}$

... interferogram: $\phi = \phi_1 - \phi_2 = \frac{4\pi}{\lambda} \Delta R$

(if $\phi_{scatt,1} = \phi_{scatt,2}$!)

ERS SAR Image

Bachu, China

approx. 100 km × 80 km

UNIVERSITY OF ALASKA FAIRBANKS

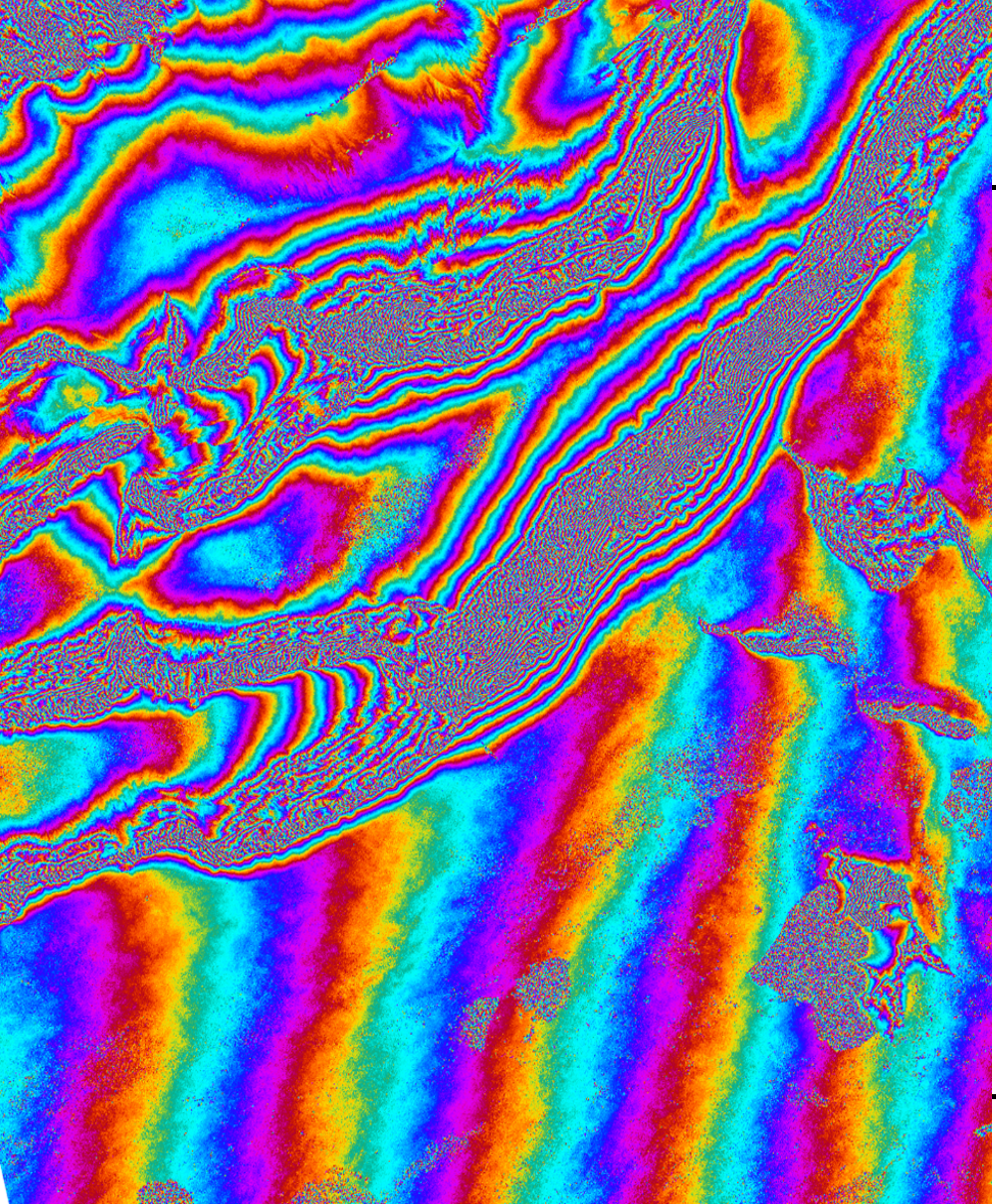

Interferometric Phase

Bachu, China

approx. 100 km × 80 km

Phase is always ambiguous w.r.t. integer multiples of 2π

color wheel

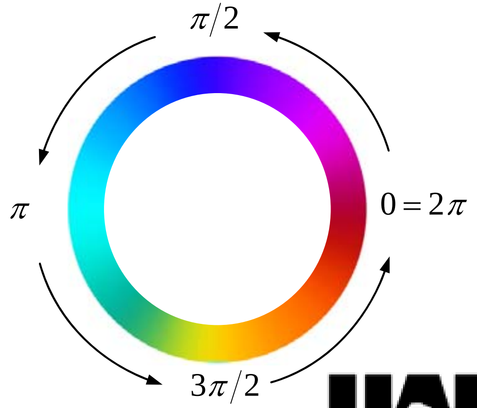

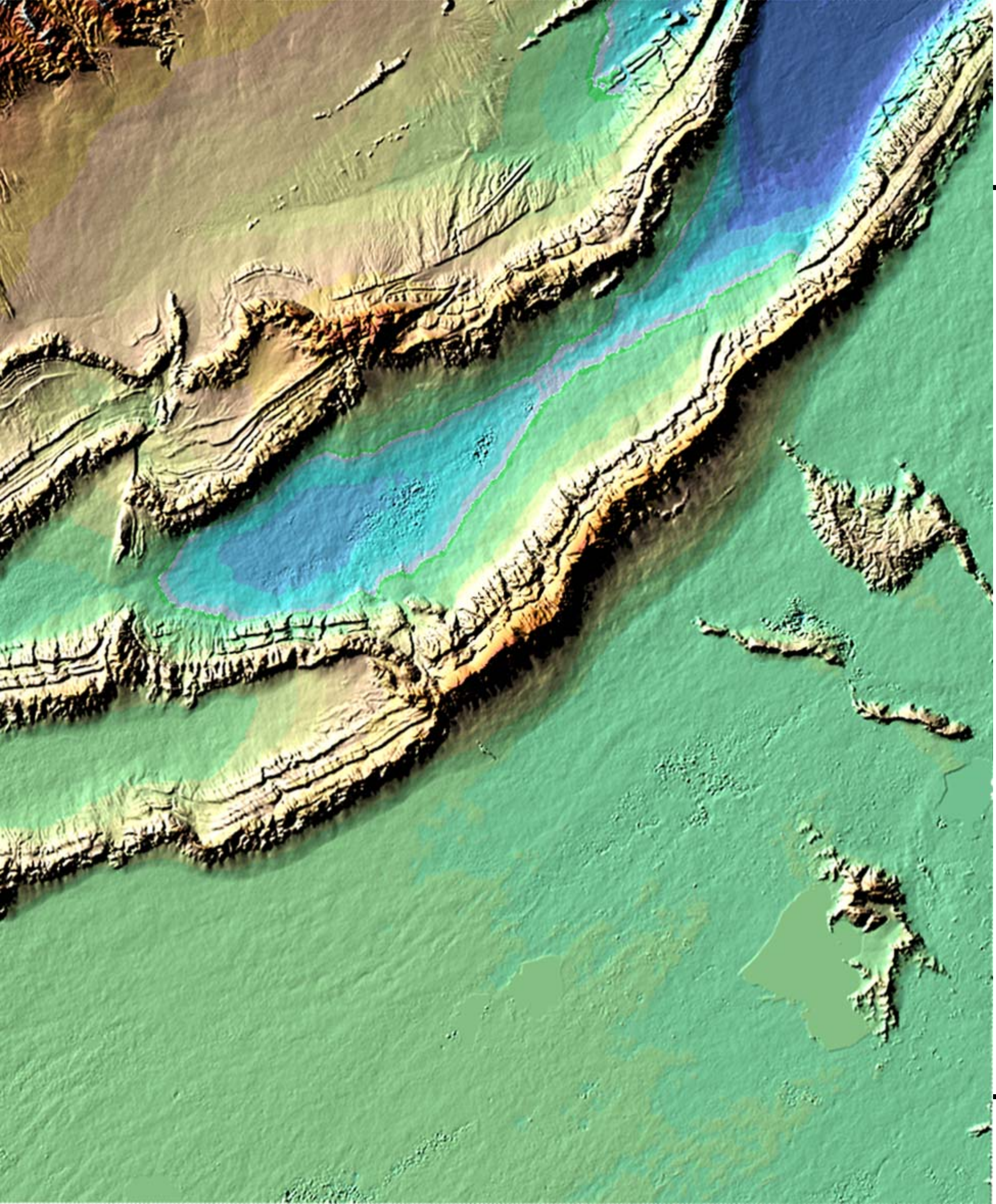

InSAR DEM (ERS-1/2)

Bachu, China

approx. 100 km × 80 km

$\phi_{scatt,1} \approx \phi_{scatt,2}$ (i.e. high coherence)

$\phi_{scatt,1} \neq \phi_{scatt,2}$ (i.e. low coherence)

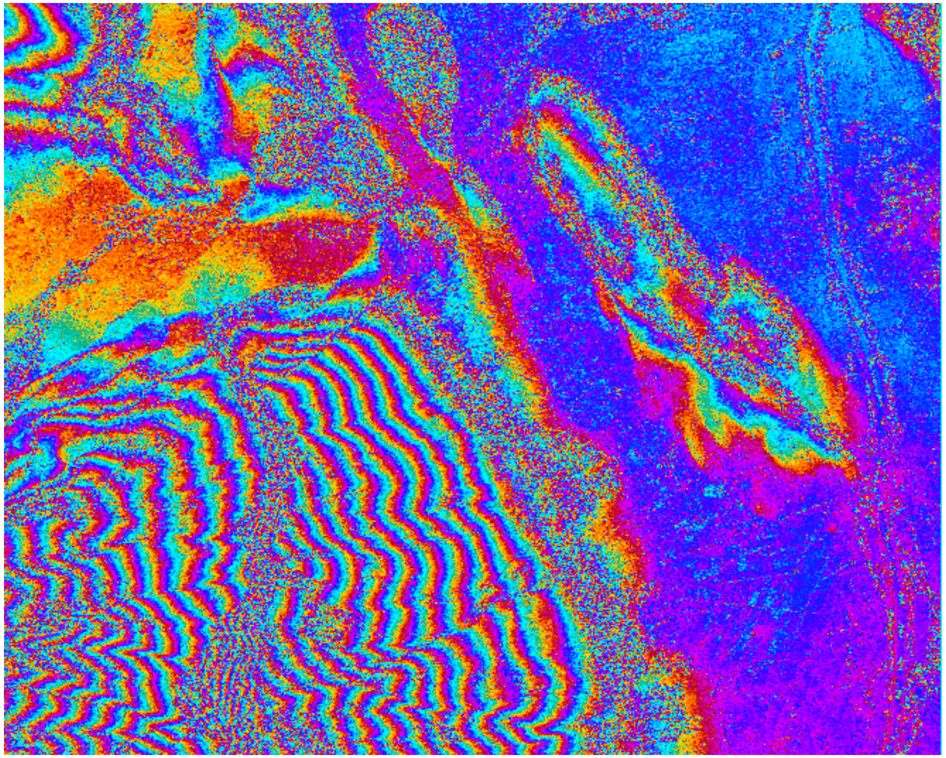

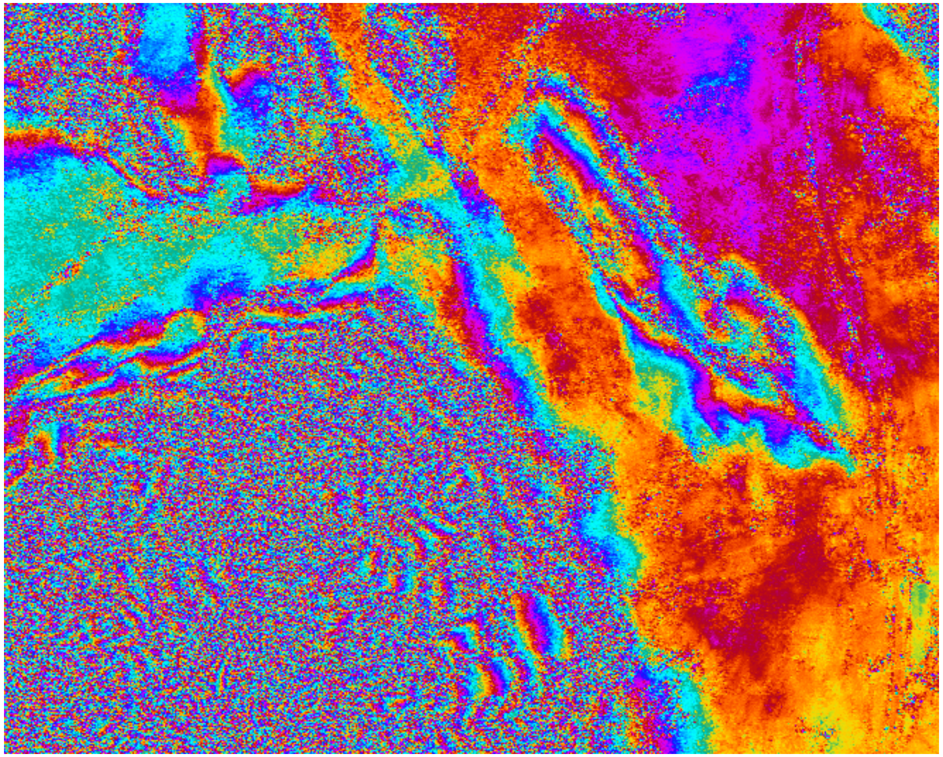

good fringe quality

13/14 Jan. 1996

bad fringe quality

23/24 March 1996

Repeat-Pass and Differential InSAR Geometry

Interferometric Phase:

$$\phi = \phi_{topo}(z;B) + \phi_{atmo} + \phi_{defo}$$

$$\phi_{defo} = \frac{4\pi}{\lambda} \Delta R_{defo}$$

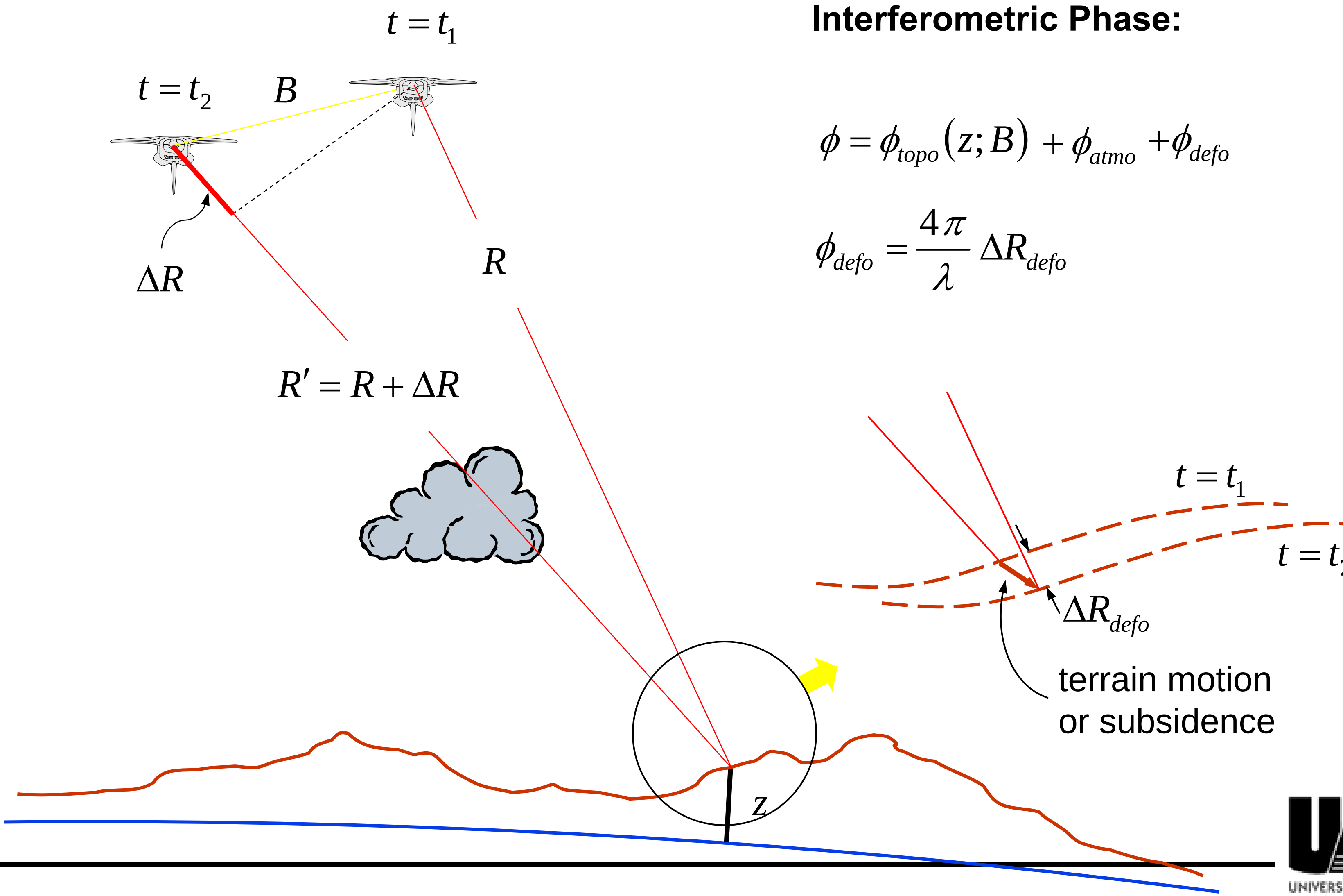

Sensitivity for Displacement

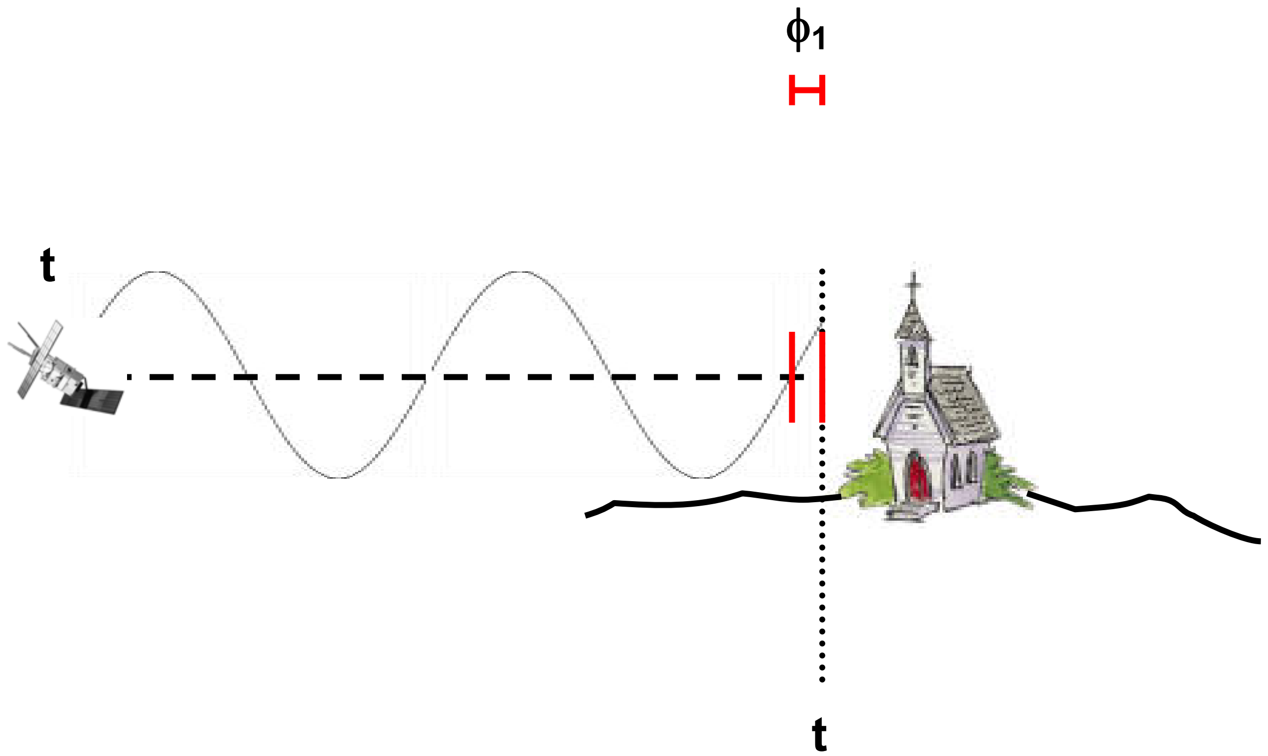

Sensitivity for Displacement

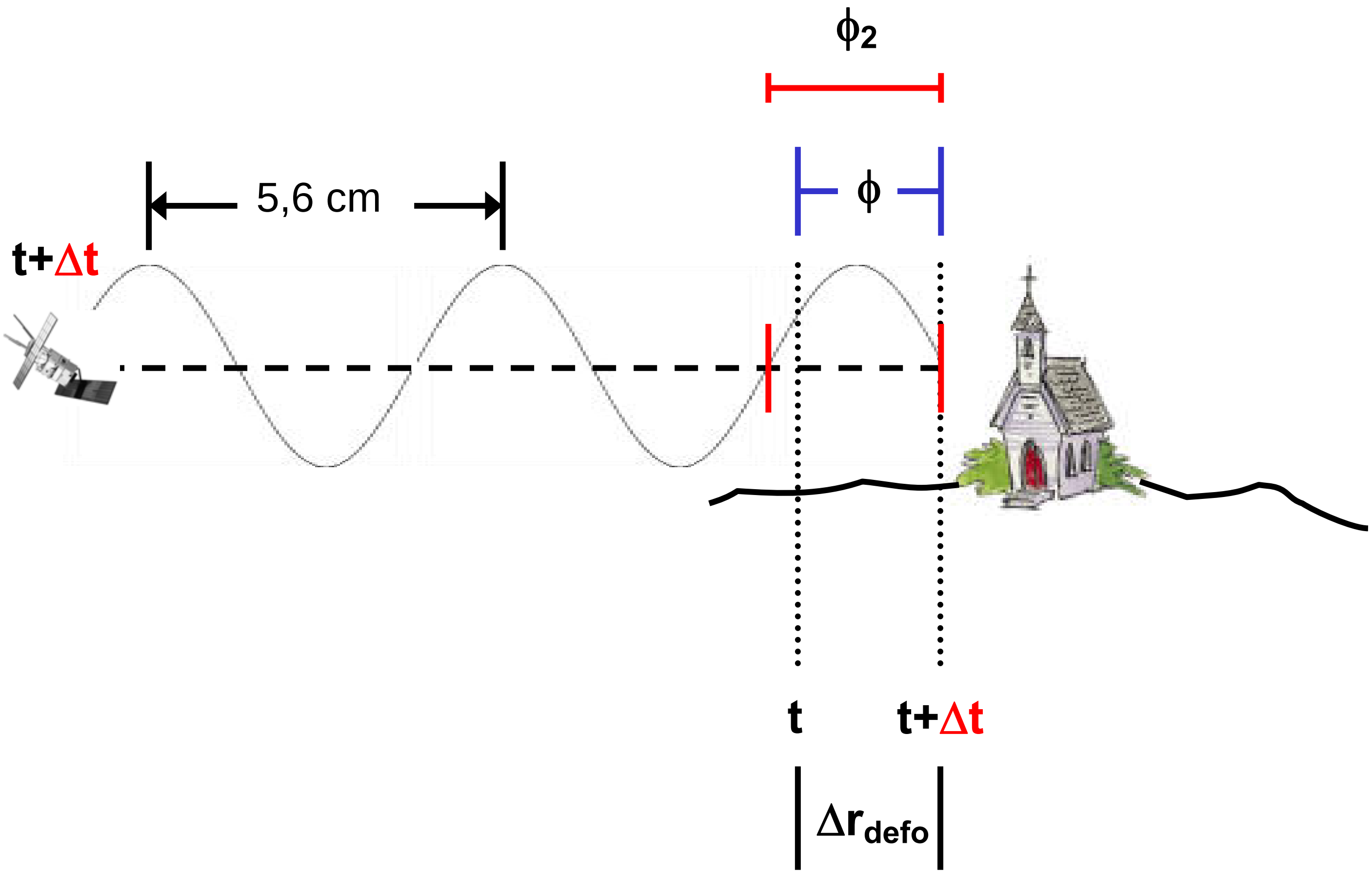

Sensitivity for Displacement

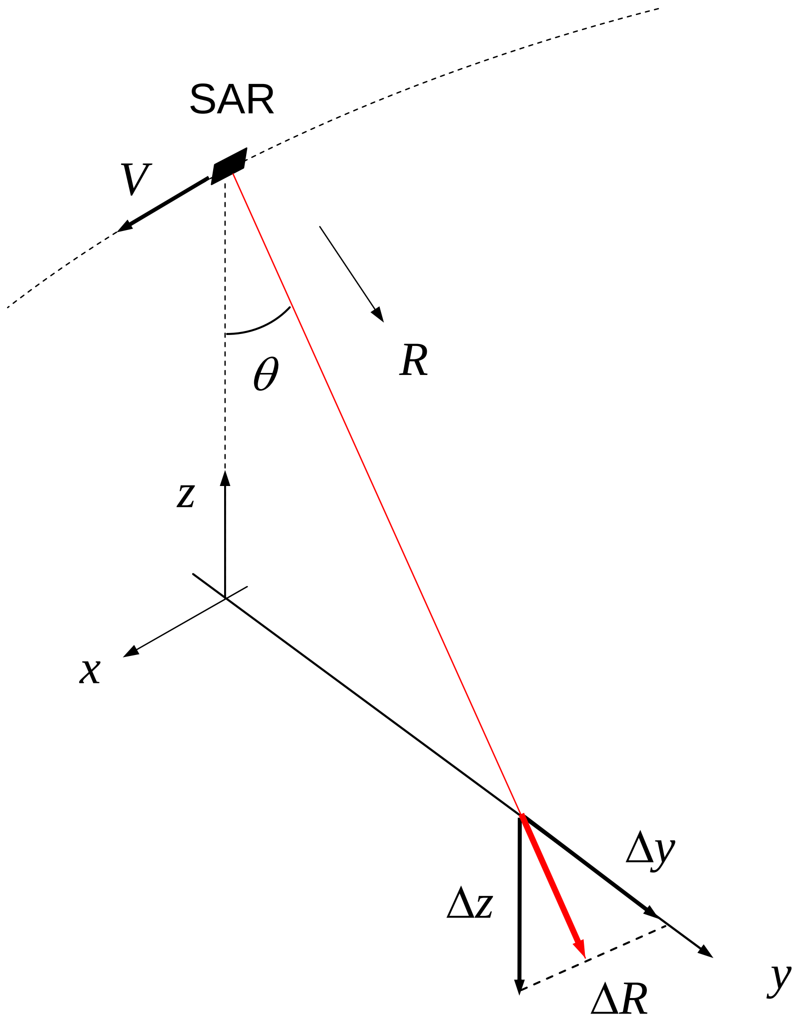

$$\Delta R = \Delta y \sin\theta - \Delta z \cos\theta$$

for ERS:

1 fringe (2π) corresponds to

2.8 cm in R

3.0 cm in z (e.g. subsidence)

7.2 cm in y (motion)

Separation of Topographic and Differential Phase

If a reliable DEM is available, use DEM to compensate for topography.

Else, ≥ 3 complex SAR images at times $t_1, t_2, ..., t_N$ are required:

Form several interferograms:

- time lag: $\Delta t_{n-m} = t_n - t_m$
- baseline: $B_{\perp, n-m}$
- phase: ϕ_{n-m}

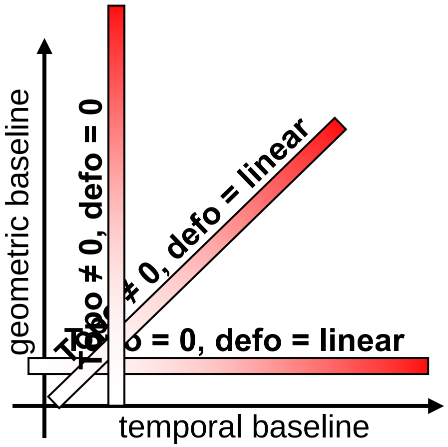

for constant velocity: $\phi_{defo} \propto \Delta t_{n-m}$ and $\phi_{topo} \propto B_{\perp, n-m}$

for singular displacement event: use $\phi_{n-m} \propto B_{\perp, n-m}$ to derive topography

Application of d-InSAR to various Geophysical Problems

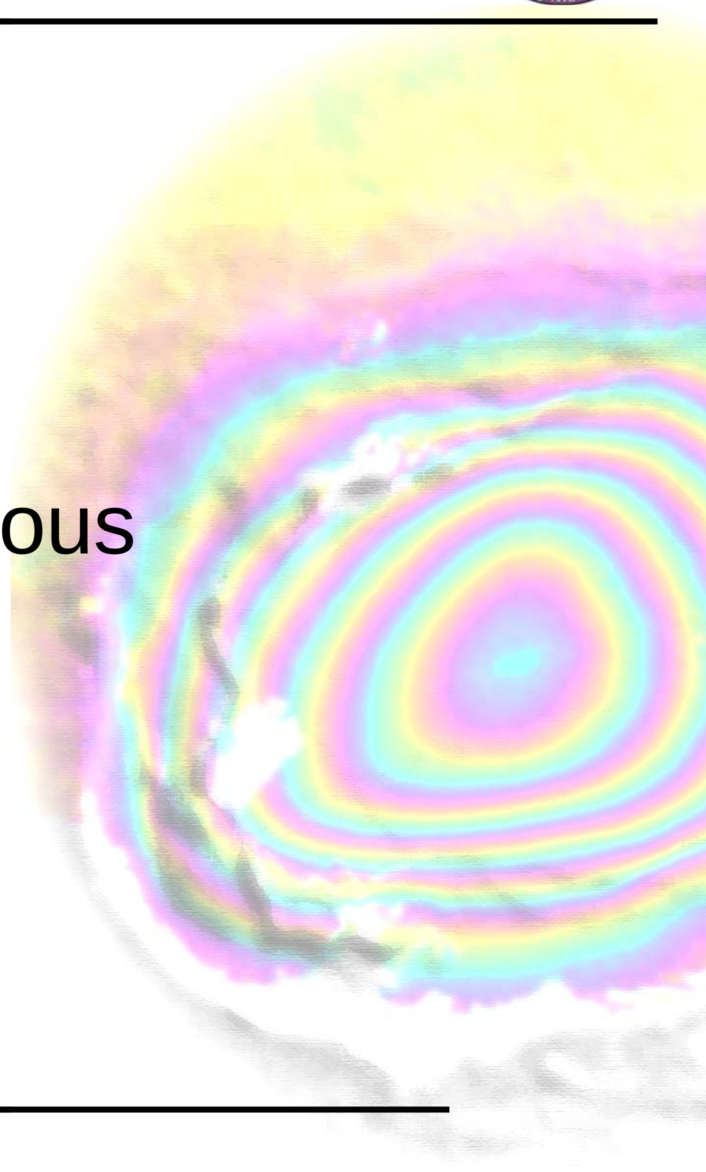

d-InSAR Displacement Pattern of an Earthquake

Izmit/Turkey, 17 August, 1999

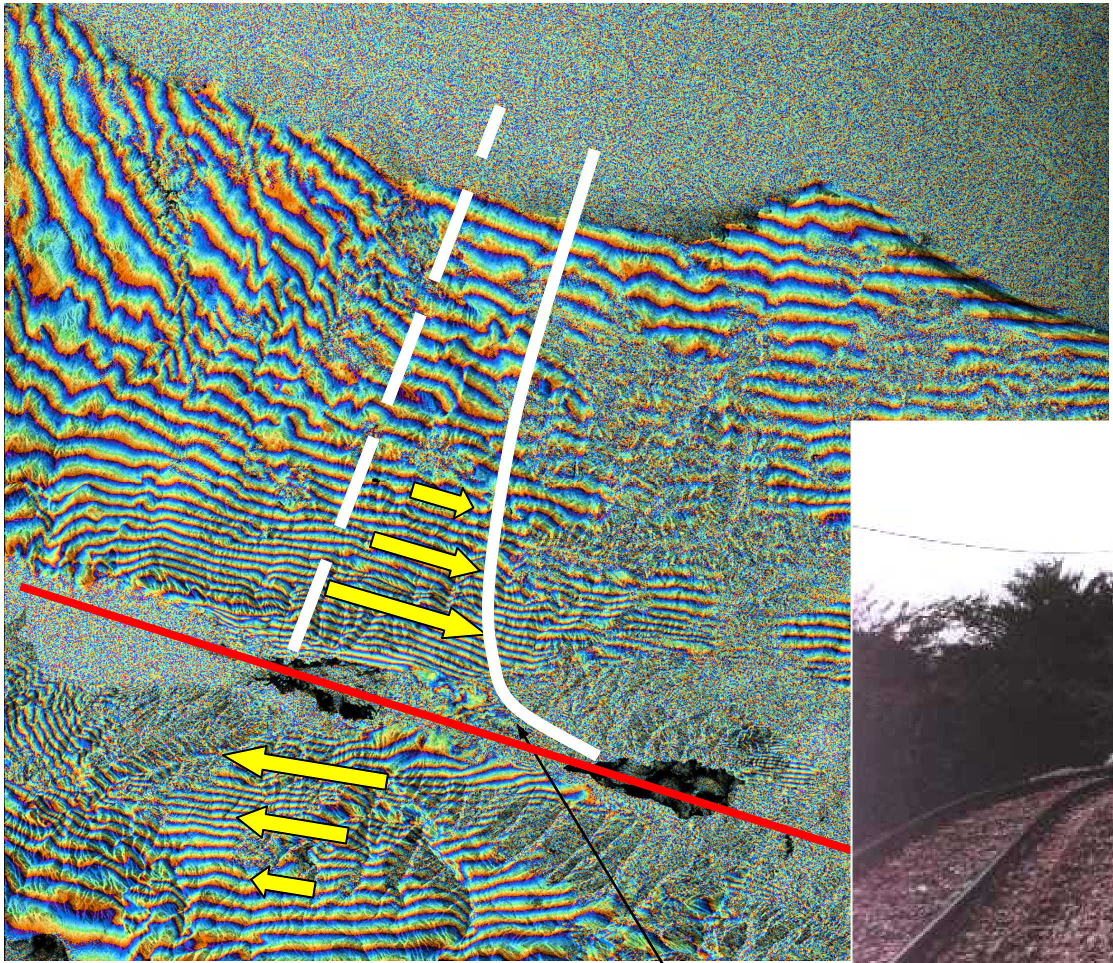

Data ERS-1/2 © ESA,
Acqusition dates: 12.08. and 16.09.1999

d-InSAR Fringe Pattern and Model

Landers Earthquake, 1993

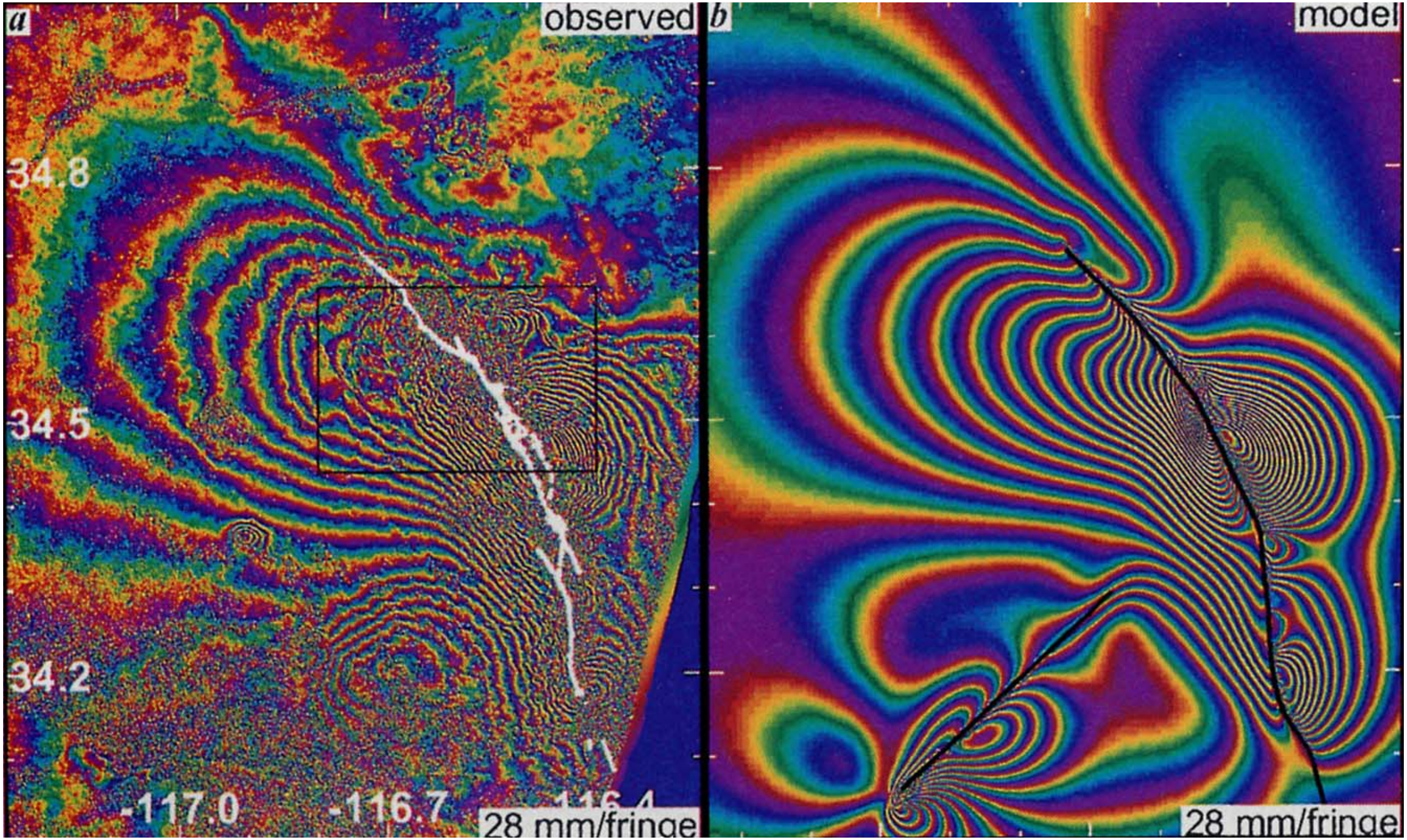

Massonnet et al, 1994

Monitoring Glacier Motion

Rutford Ice Stream, Antarctica

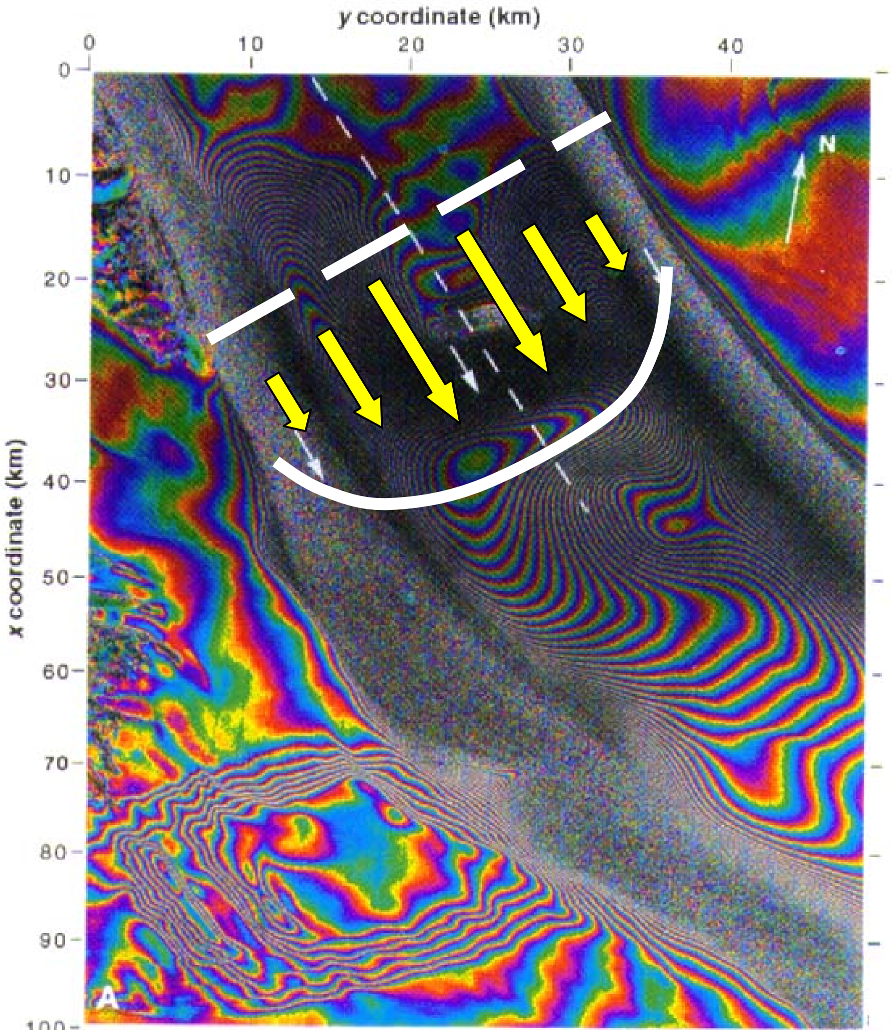

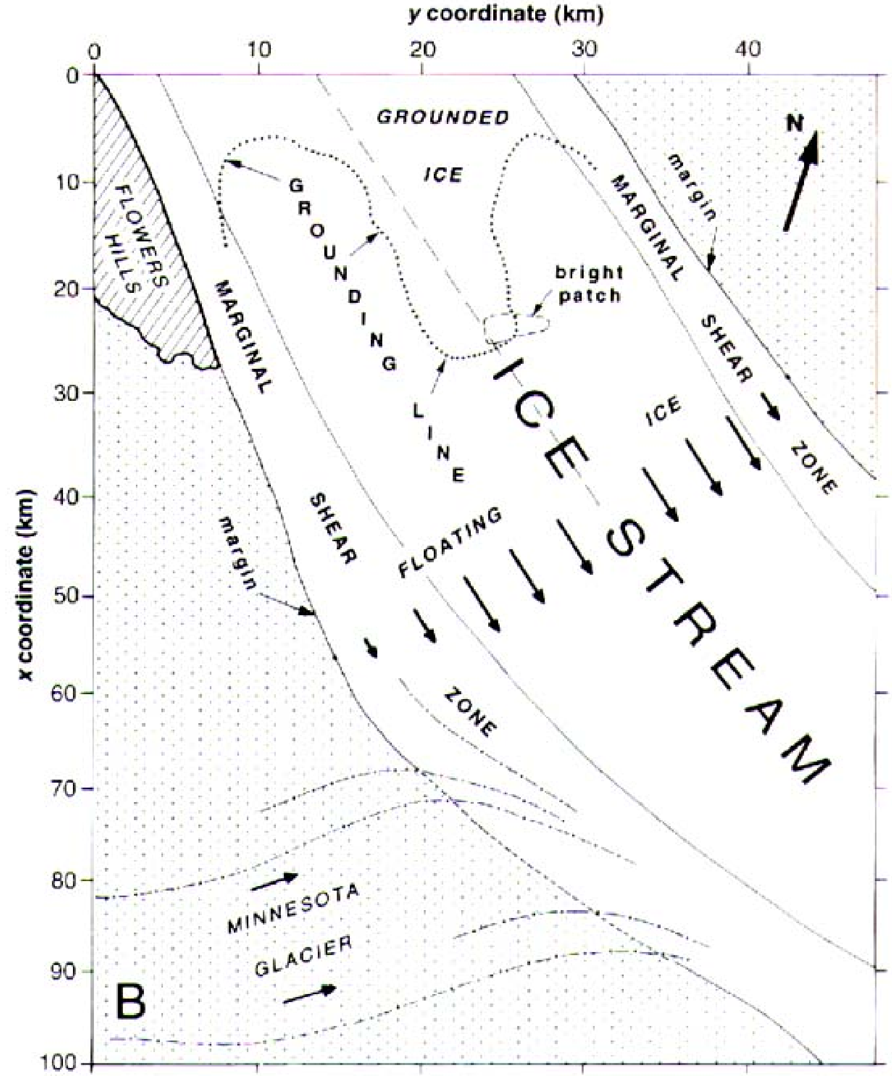

Glacier Flow Field Derived from d-InSAR

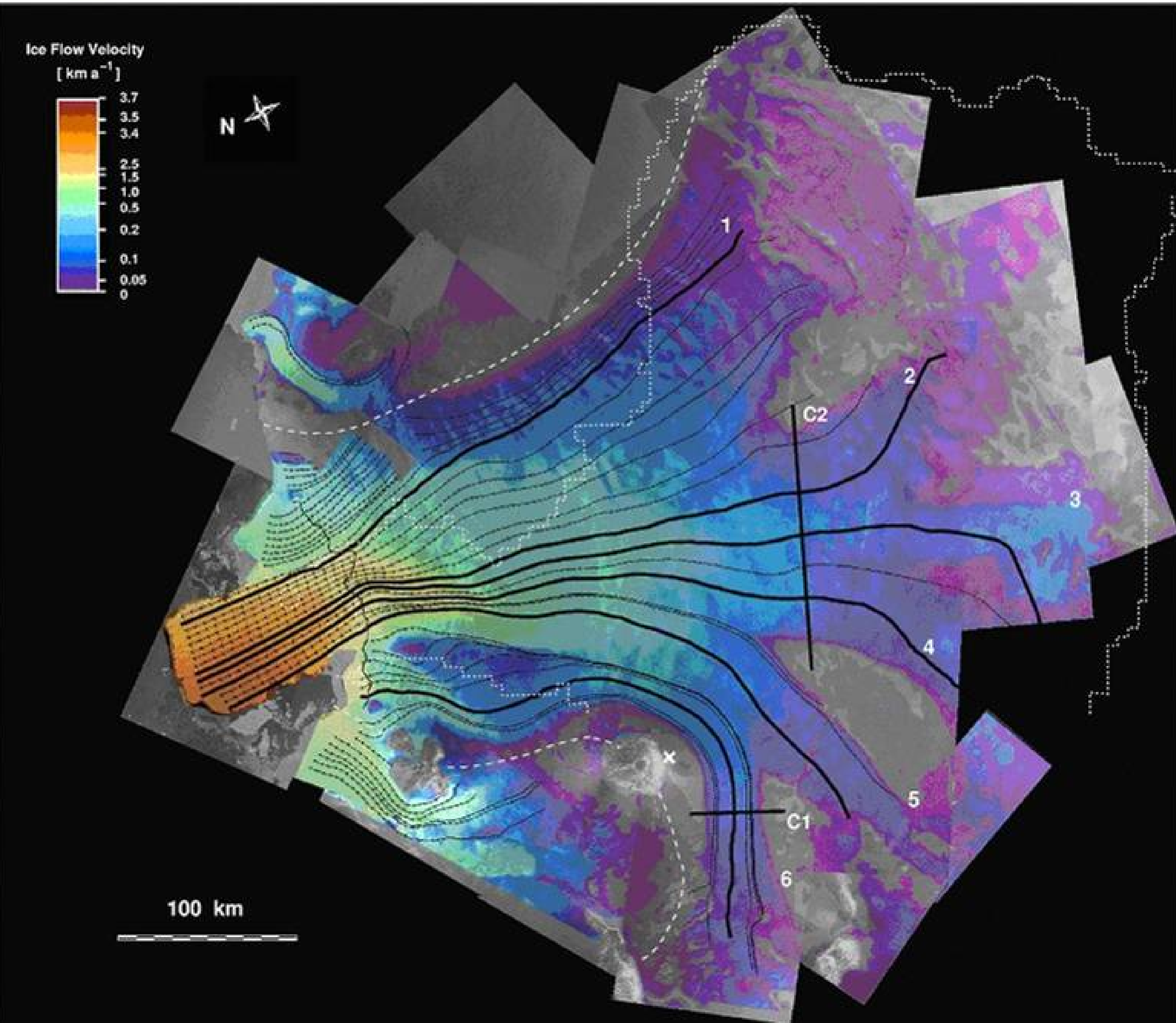

Antarctic Thwaites glacier

approx. 500 km x 500 km

(Lang et al., 2003)

Glacier Flow Field Derived from d-InSAR

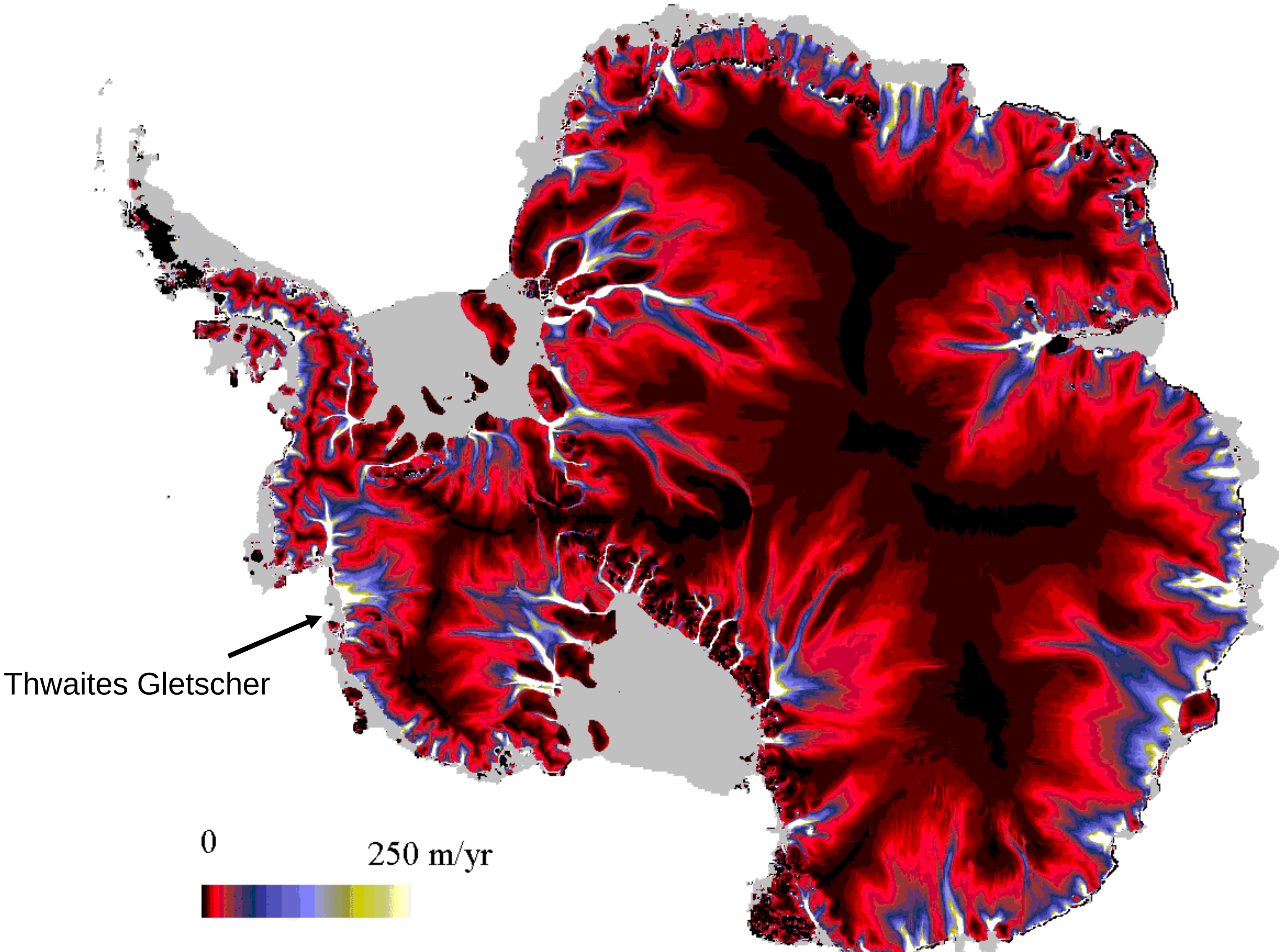

Monitoring Mount Peulik, Alaska with d-InSAR

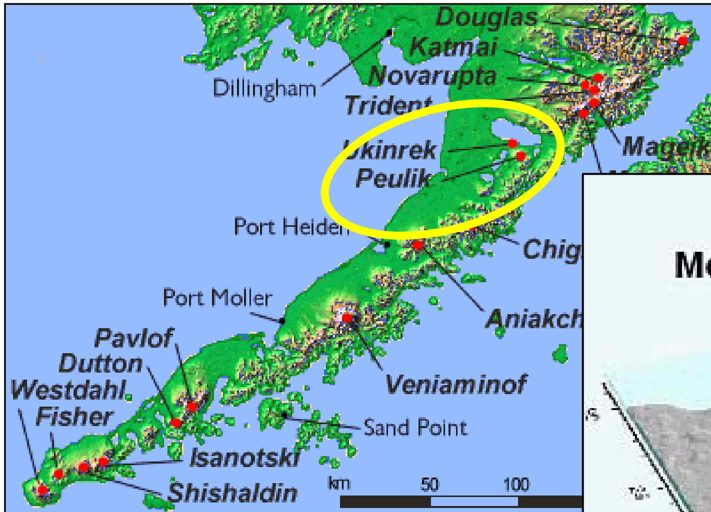

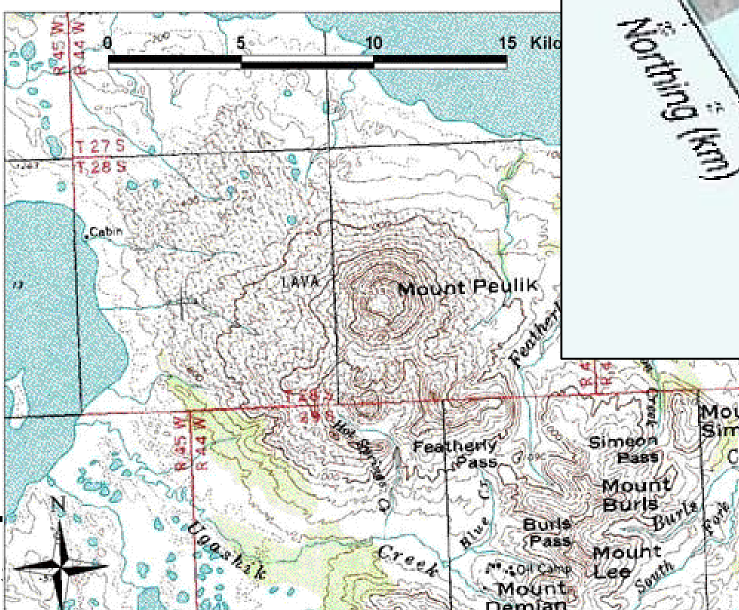

17 cm inflation, Sept. 1996 to Oct. 1997

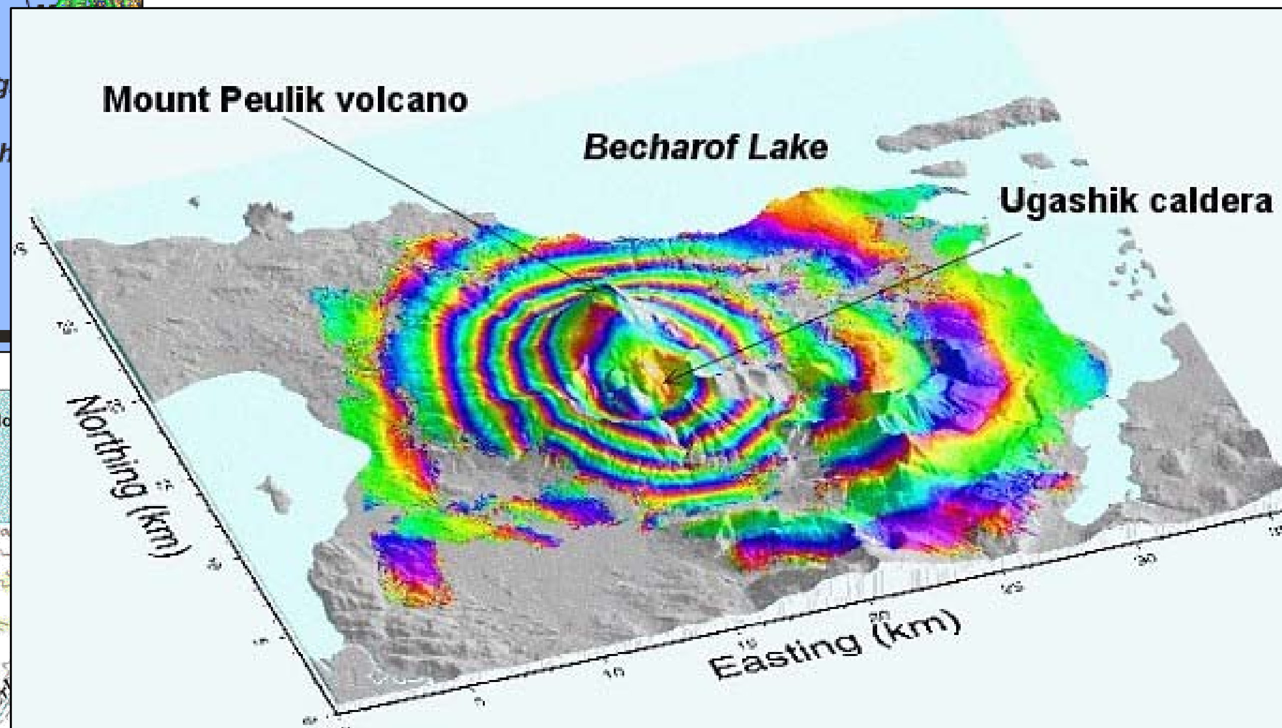

Z. Lu, C. Jr. Wicks, D. Dzurisin, J.A. Power, S. Moran, W. Thatcher, (2001)

Monitoring Westdahl Peak, Alaska with d-InSAR

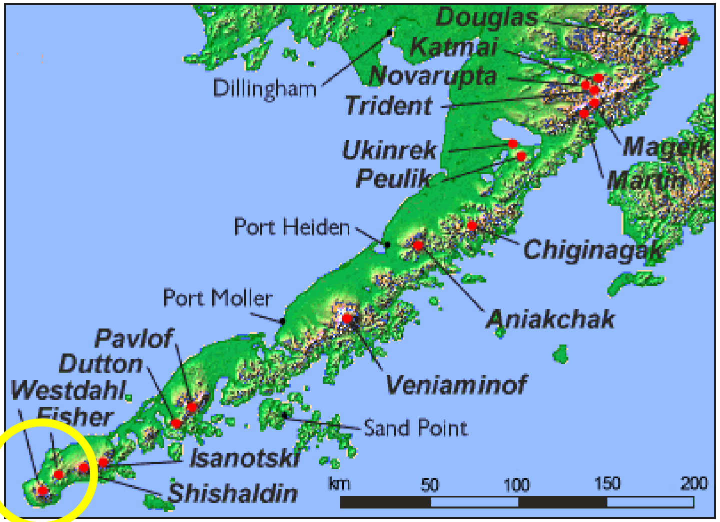

15 cm inflation of Westdahl Peak, Alaska between Nov. 92 and Nov. 98

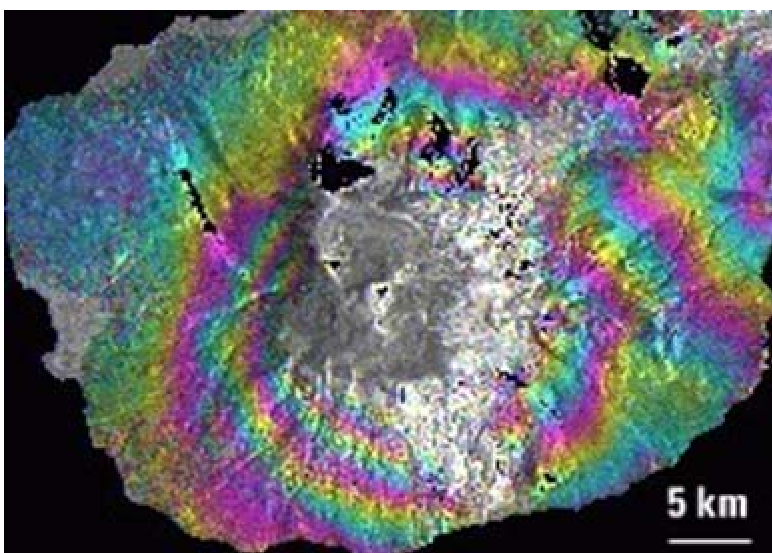

d-InSAR results

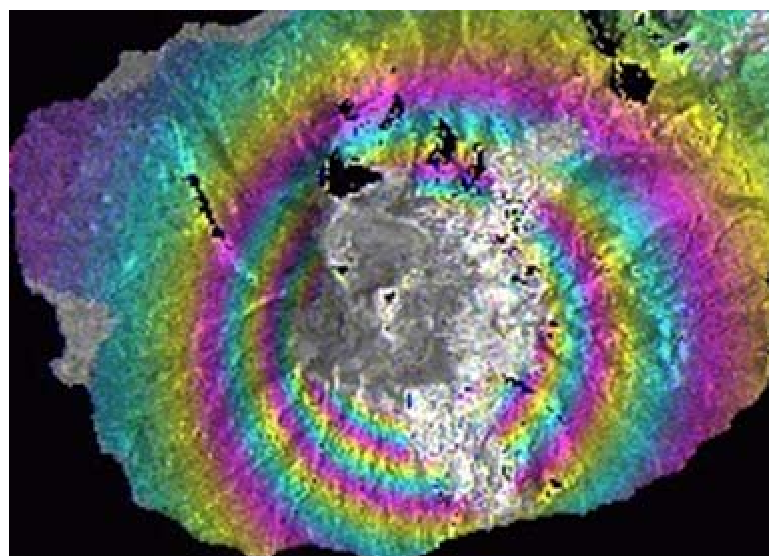

geophysical model

UNIVERSITY OF ALASKA FAIRBANKS

Monitoring Galapagos Islands with d-InSAR

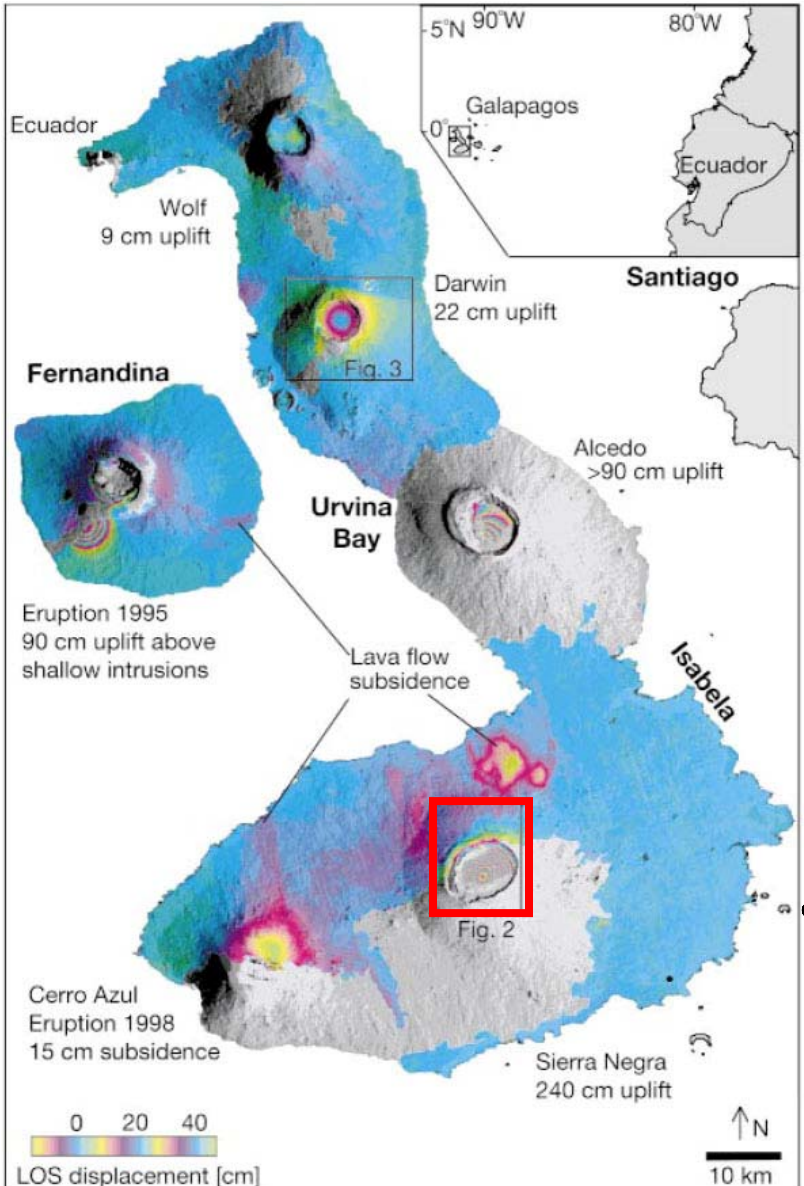

F. Amelung et al, Nature 2000

Deformation fringes over time

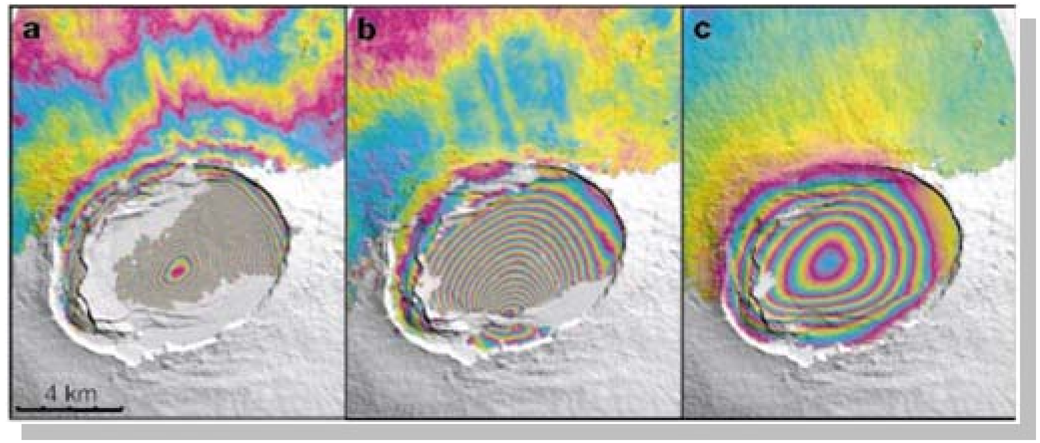

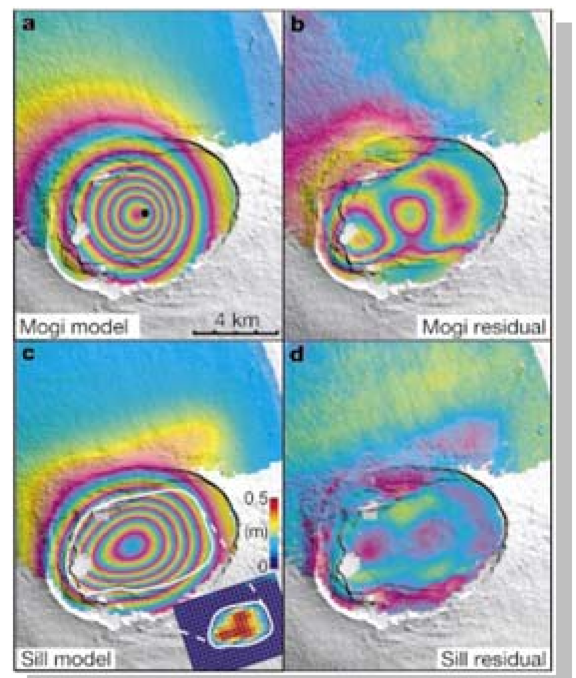

model results and phase residuals for mogi and sill model

Tidal Fringes in SAR Interferograms

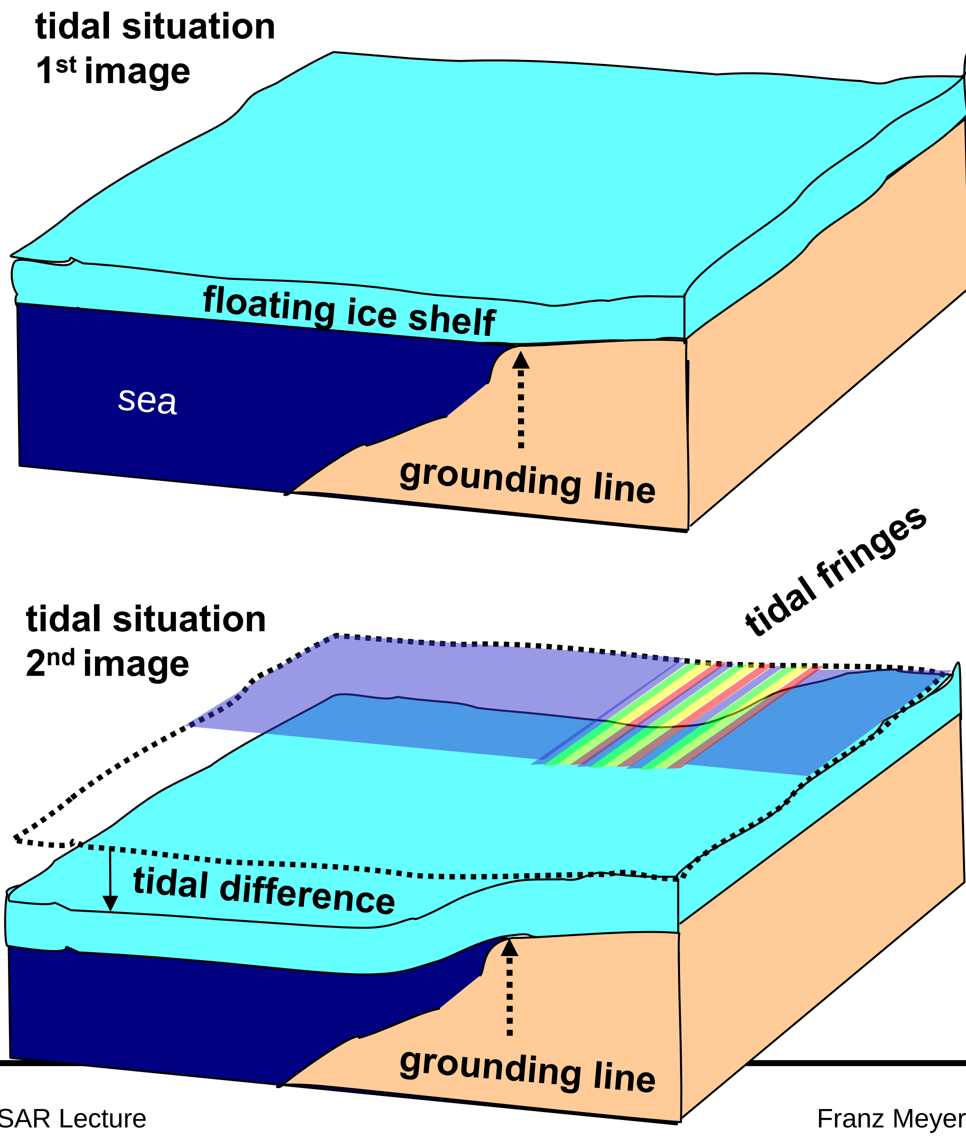

double difference interferogram

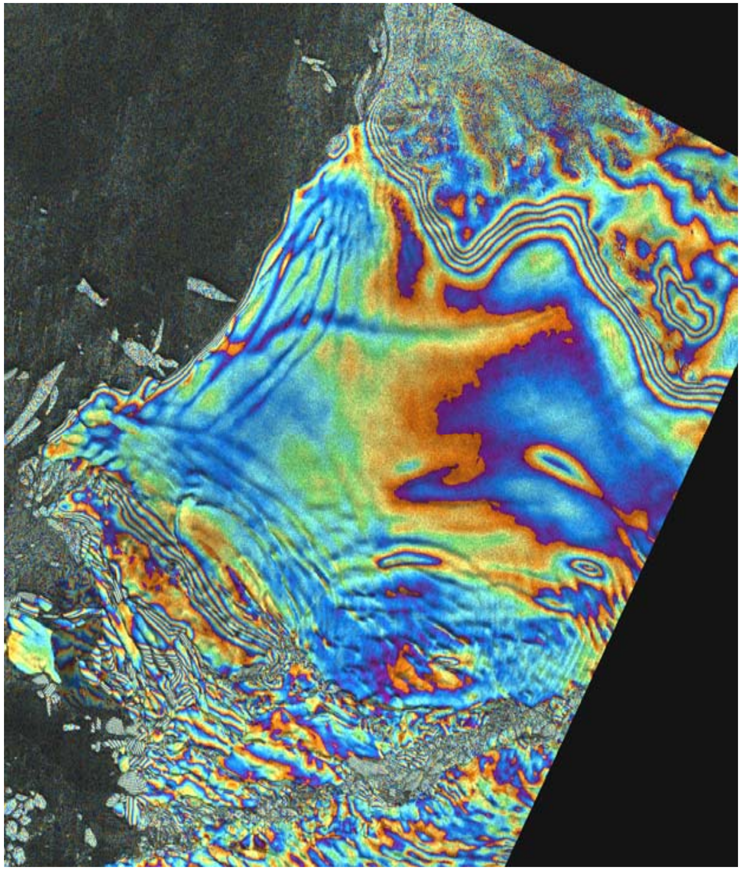

Amundsen Sea, West Antarctica

B. Rabus, O. Lang, DFD
Data: ERS-1/2 ©ESA

Limitations of d-InSAR

D-InSAR Limitations

- No separation of
  - Atmospheric effects
  - Orbit errors
  - Deformation

- Temporal baseline limited due to
  - Temporal decorrelation
  - Phase unwrapping

- Spatial baseline limited due to
  - Height ambiguities
  - Spectral decorrelation

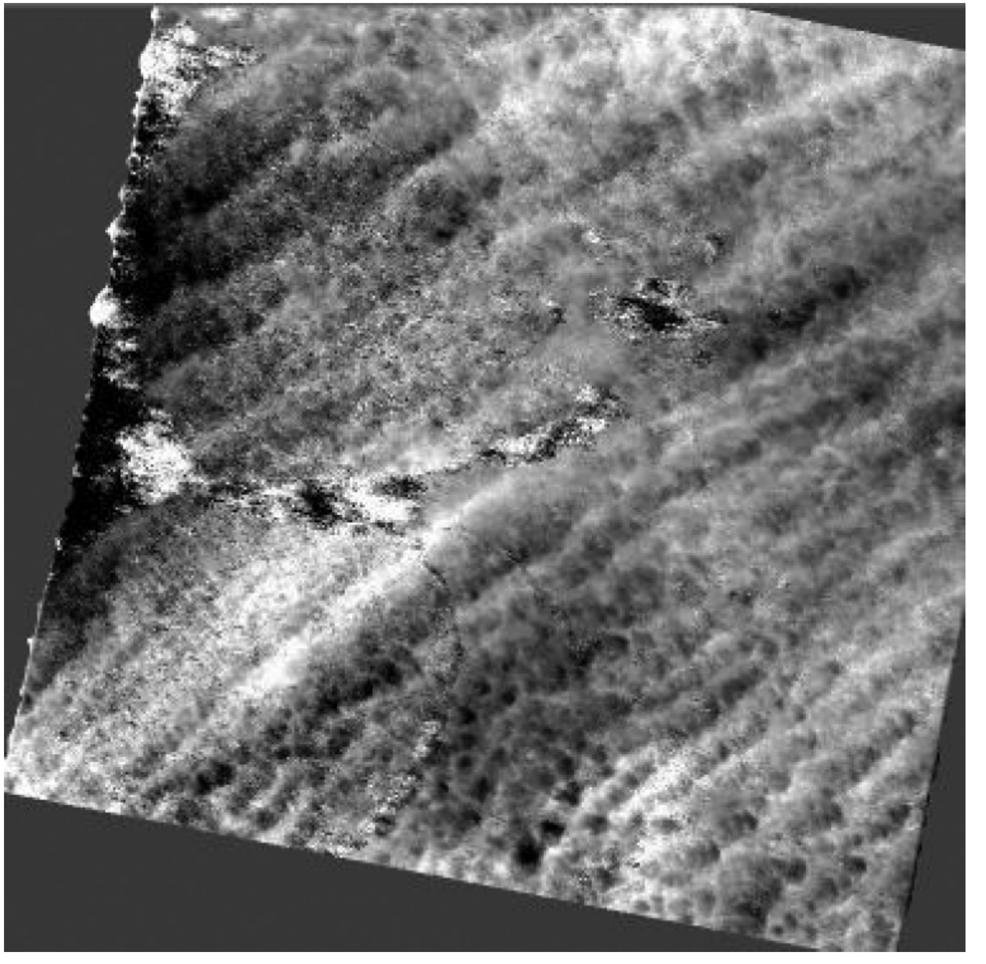

D-InSAR Limitations

- No separation of
  - Atmospheric effects
  - Orbit errors
  - Deformation

- Temporal baseline limited due to
  - Temporal decorrelation
  - Phase unwrapping

- Spatial baseline limited due to
  - Height ambiguities
  - Spectral decorrelation

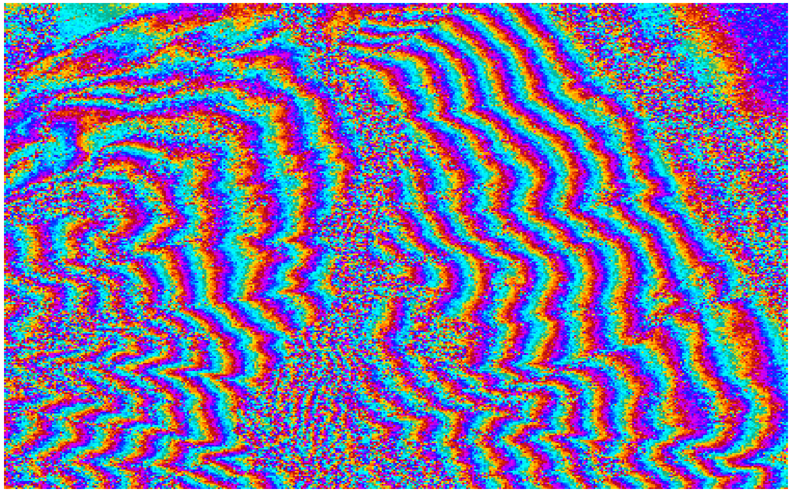

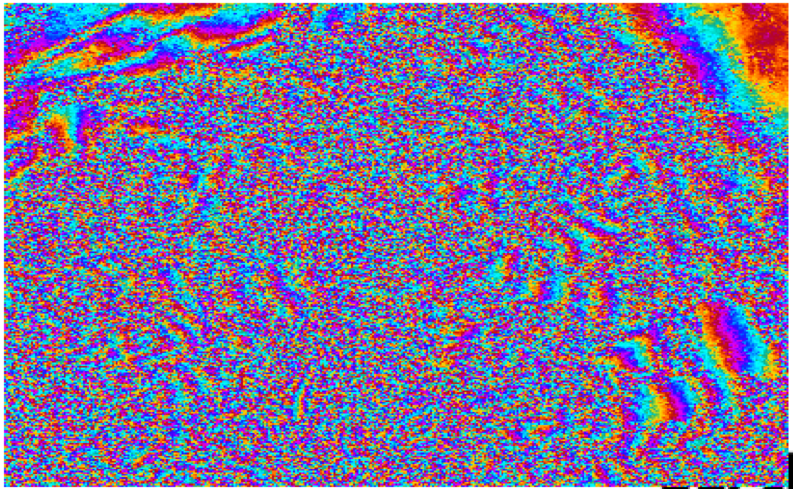

D-InSAR Limitations

- No separation of
  - Atmospheric effects
  - Orbit errors
  - Deformation
- Temporal baseline limited due to
  - Temporal decorrelation
  - Phase unwrapping
- Spatial baseline limited due to
  - Height ambiguities
  - Spectral decorrelation

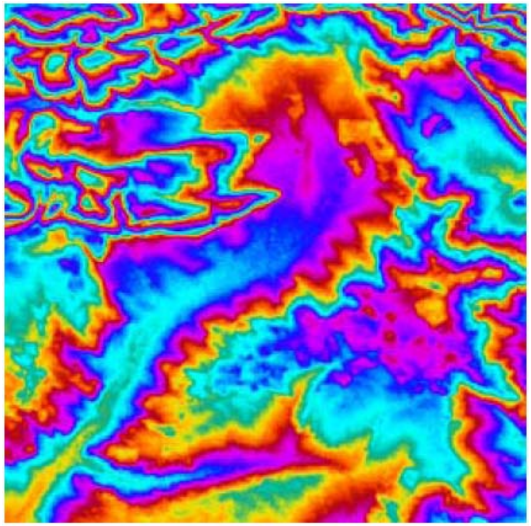

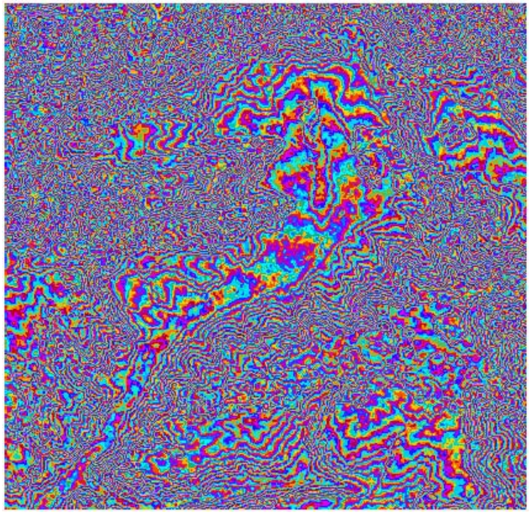

Spatial Ground Frequencies vs. Signal Frequencies

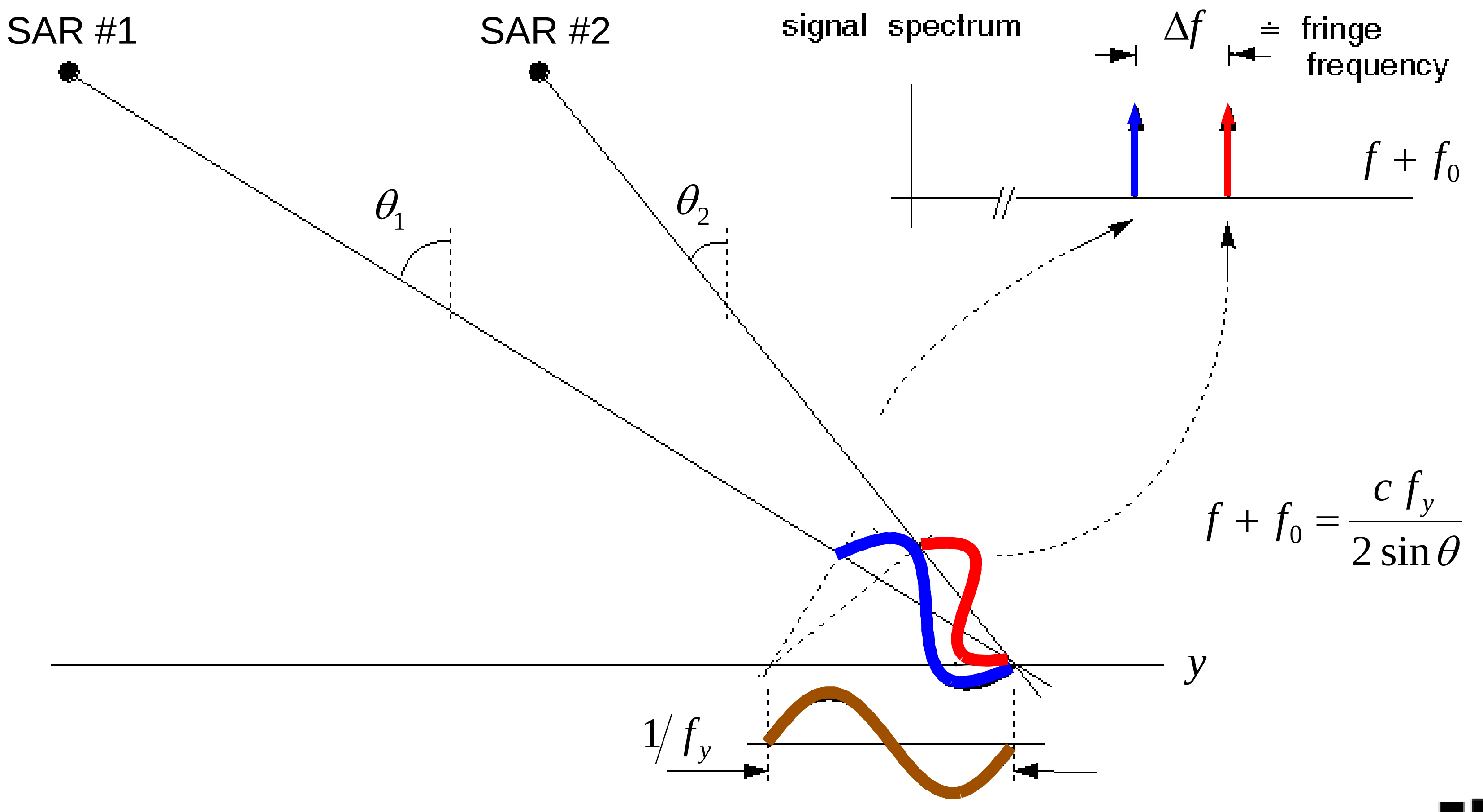

Spatial Ground Reflectivity Spectrum vs. Signal Spectrum

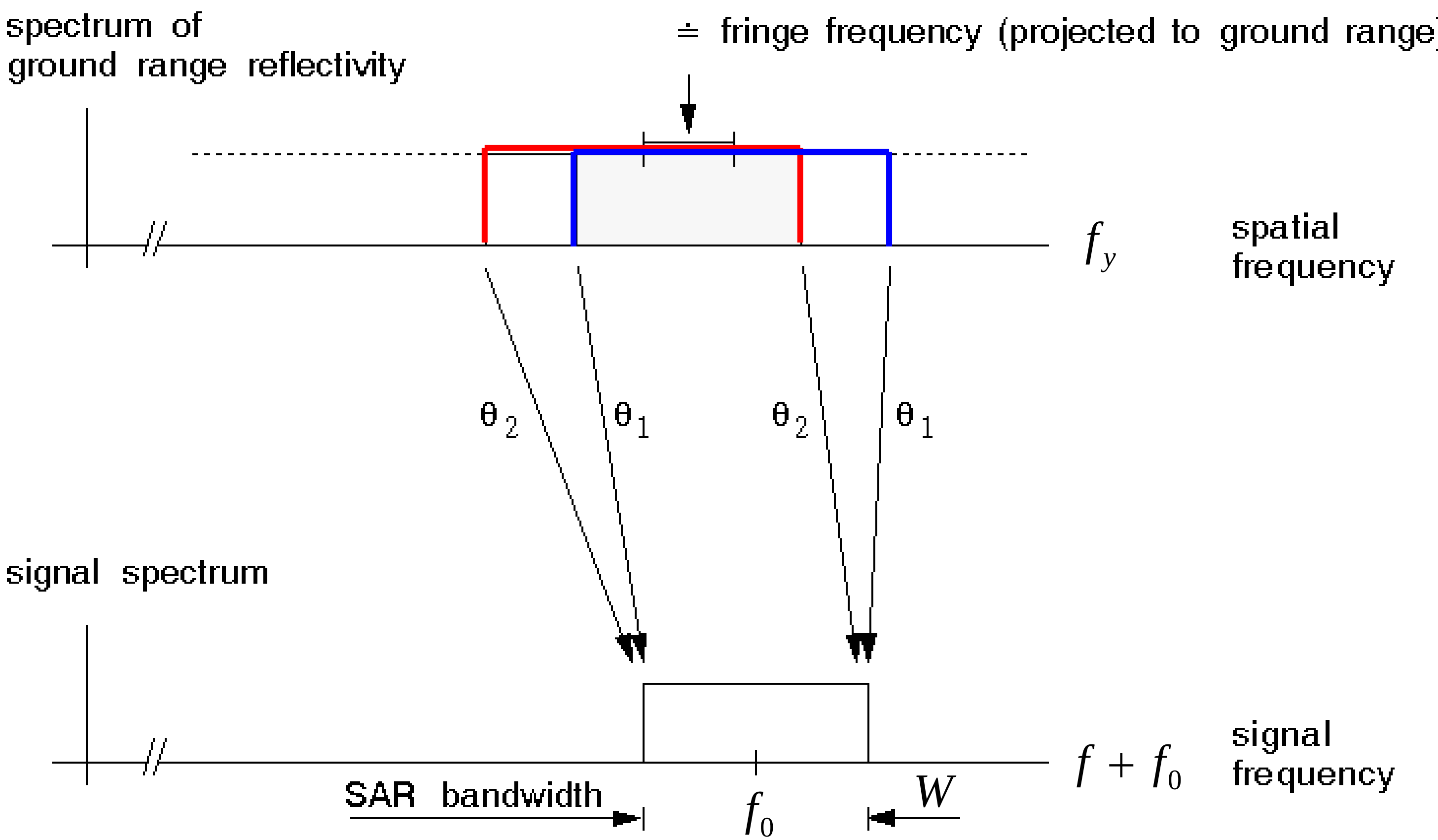

Spectral shift filtering: cut off non-overlapping spectral bands

An Introduction to Persistent Scatterer Interferometry (PSI)

Persistent Scatterer Interferometry (PSI)

- Invented by Alessandro Ferretti, Fabio Rocca, and, Claudio Prati, Polytechnical University of Milan, Italy

incoherent average of 70 ERS SAR images

individual images (9 years)

Persistent Scatterer Interferometry

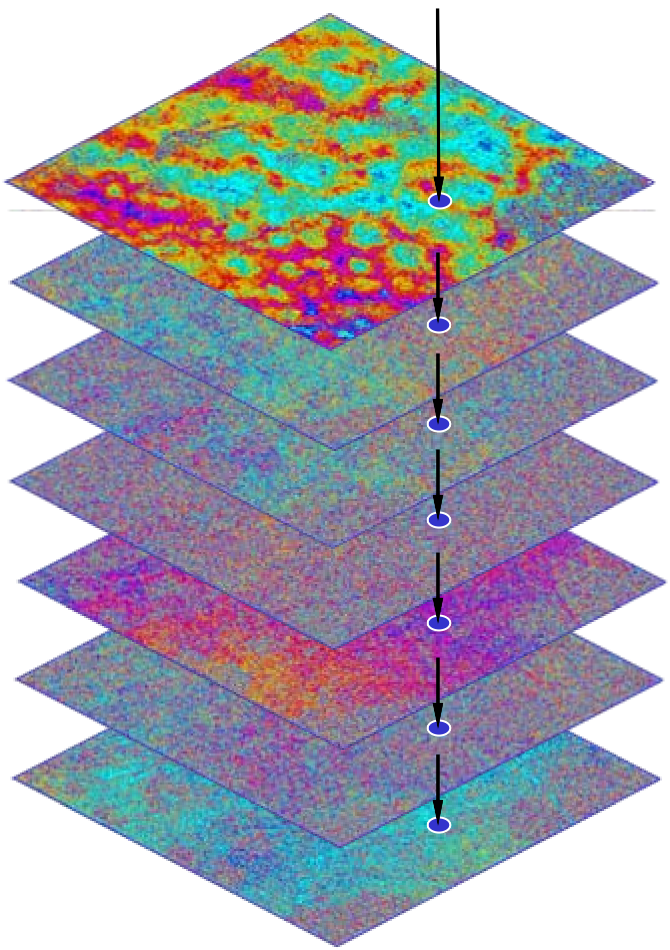

- Many interferograms
- Identification of isolated stable points
- Temporal phase analysis
- Allows separation of atmosphere and deformation
- Detectable velocities from cm/day to mm/year

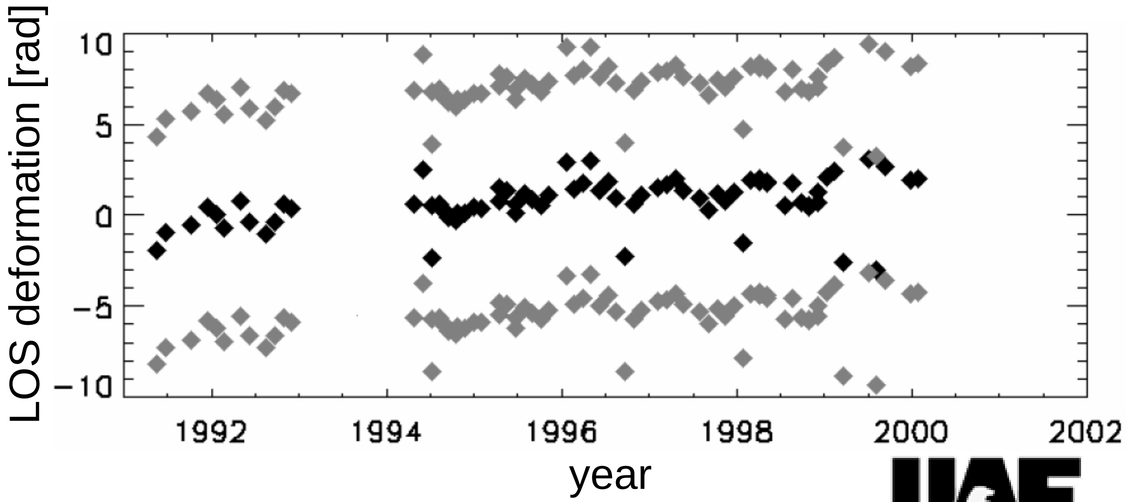

Scatterer Types in a SAR Image

- Distributed targets
- Point like scatterers
  - Corner reflectors
  - Permanent scatterers (point scatterer of opportunity)

Scattering Characteristics

Distributed Targets

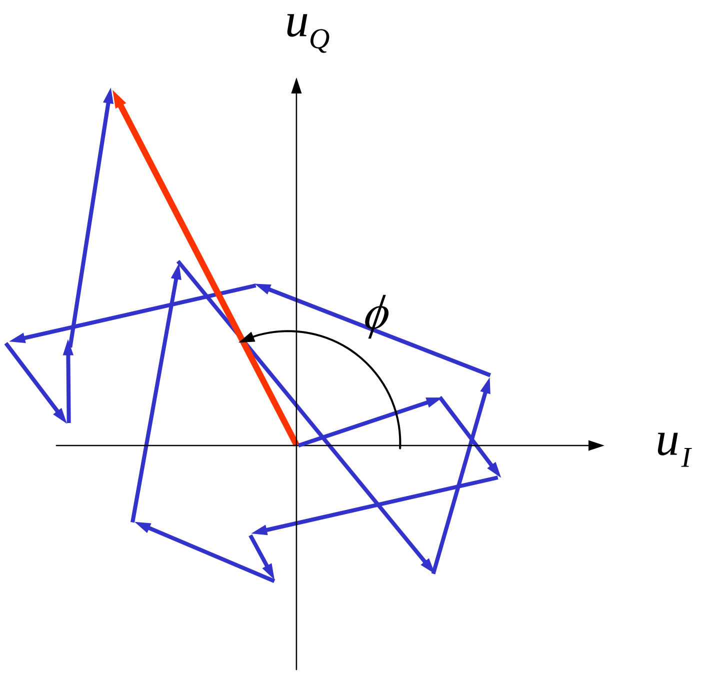

Point Targets

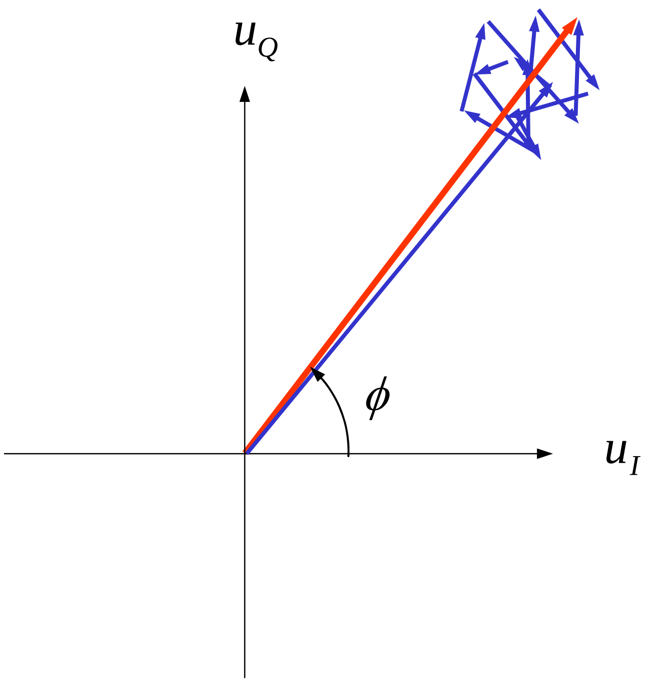

Processing Chain

CEOS CD

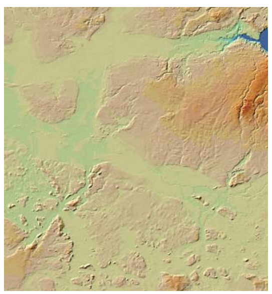

DEM

data import

InSAR processing

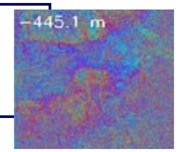

D-InSAR processing

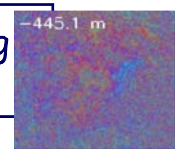

estimation

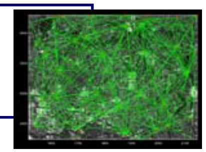

visualization

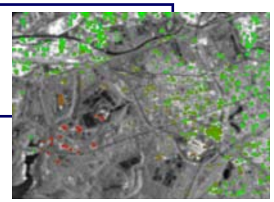

v(t, rg, az)
Δh(rg,az)
atmospheric delay

calibration

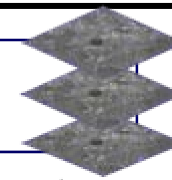

PS detection

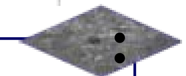

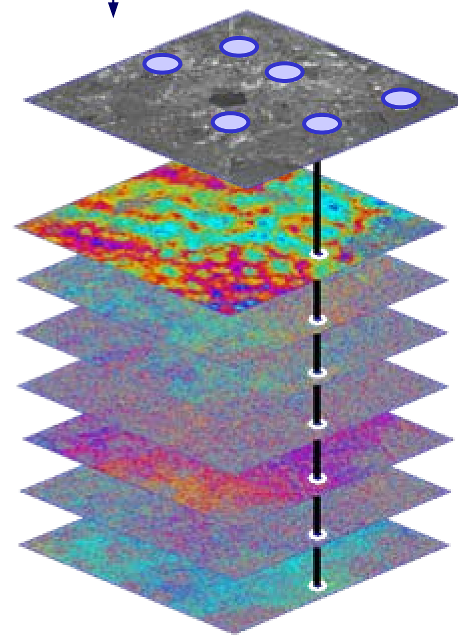

Persistent Scatterer Interferometry

- Phase of an interferogram:

Estimation by model inversion | **Estimation by residual analysis**

$$\phi = \phi_{topo} + \phi_{defo} + \phi_{atmo} + \phi_{noise}$$

- ϕ_{topo}: proportional to spatial baseline
- ϕ_{defo}: proportional to temporal baseline
- ϕ_{atmo}: random in time – smooth in space
- ϕ_{noise}: random in time – random in space

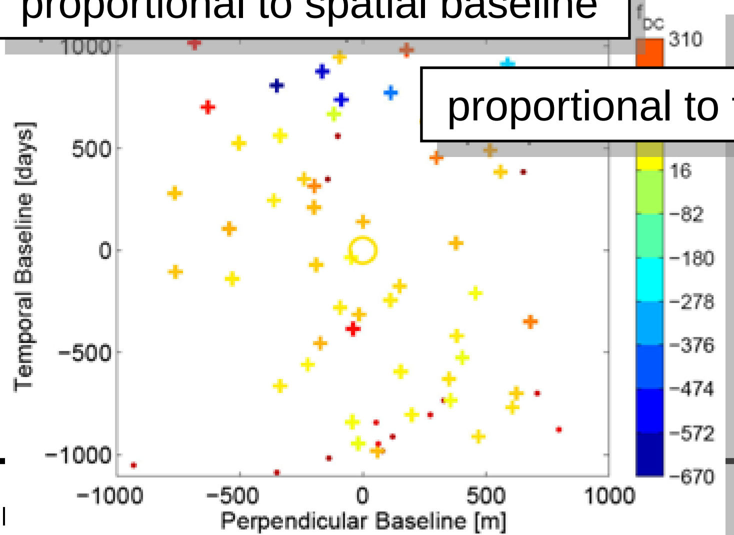

PSI Examples

Test Site Berlin, Germany

Berlin
1991 - 2000

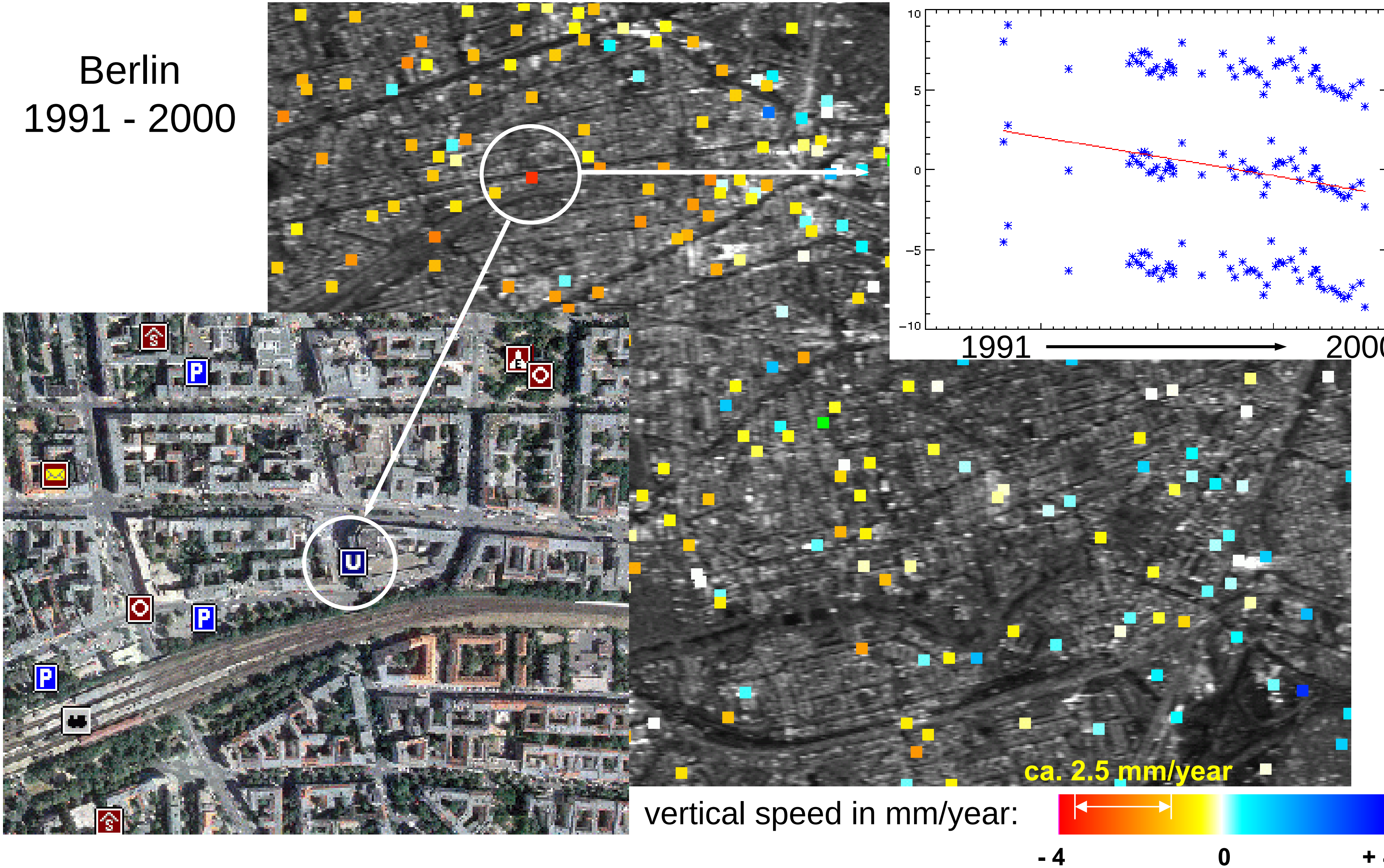

Test Site Berlin, Germany

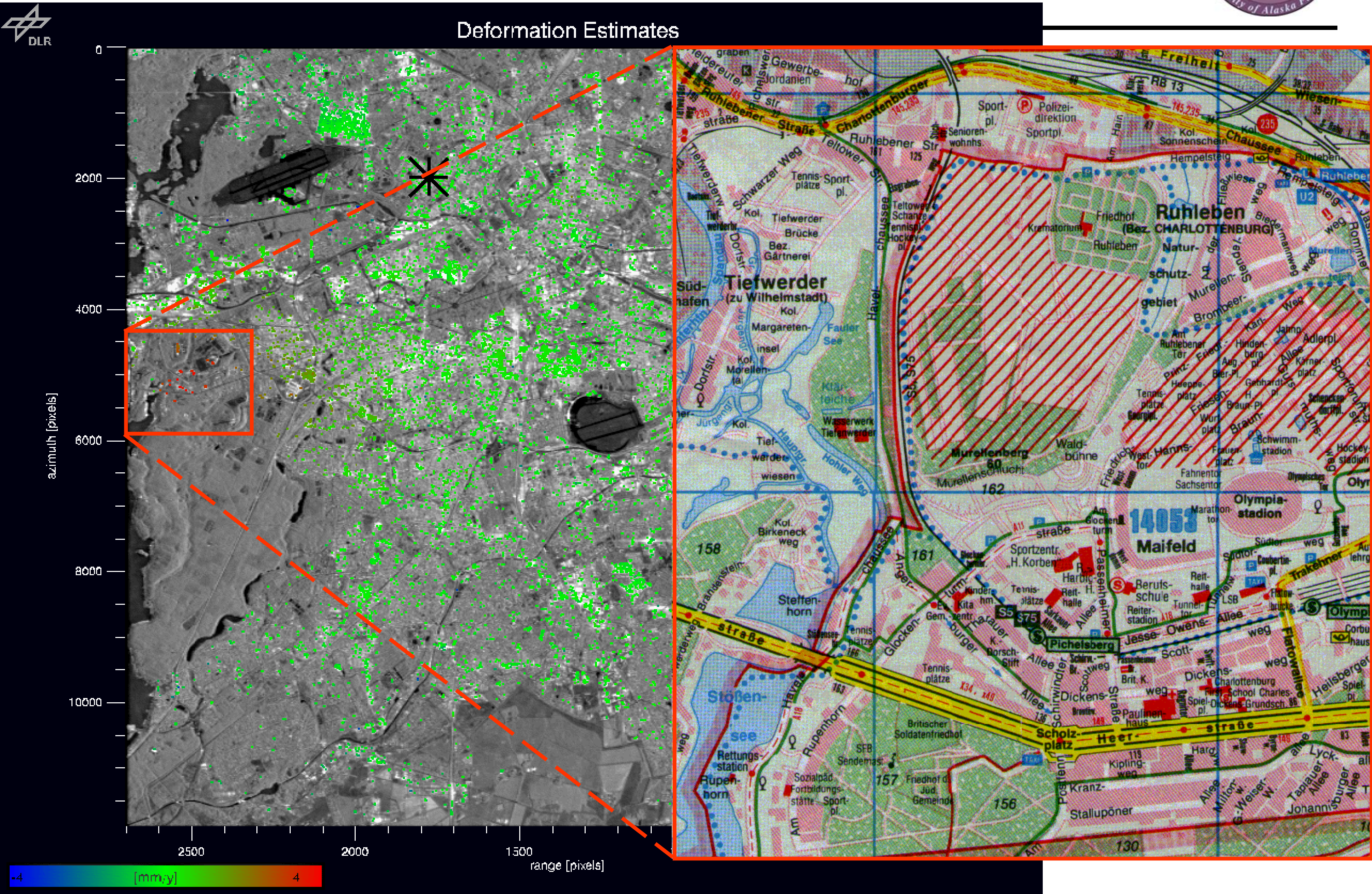

Interpolated Deformation from PS InSAR

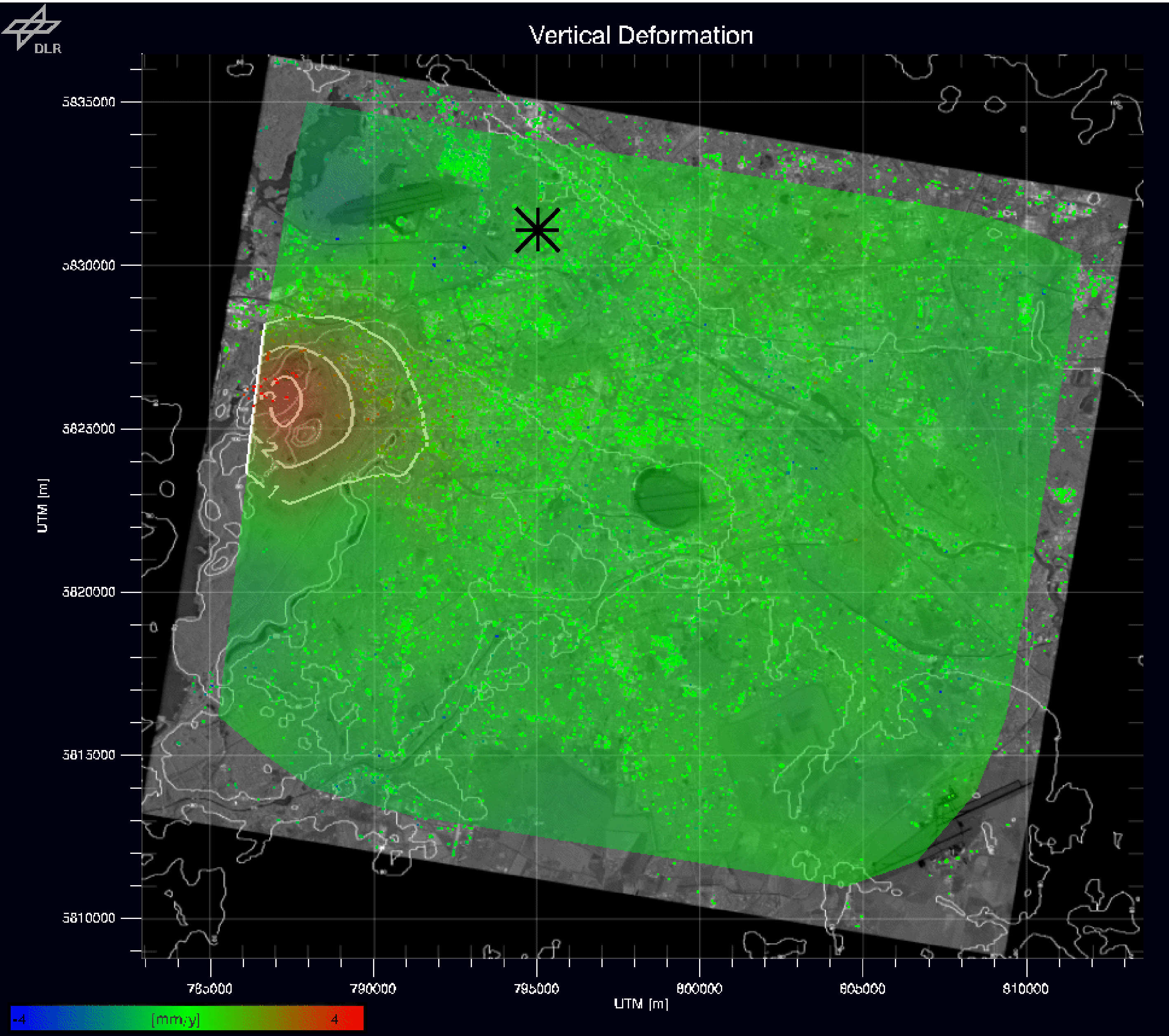

Deformation Field Berlin

red:
uplift by 4 mm/year due to ground water regulation

70 ERS-1/2 images

1992 - 2001

Periodic Seasonal Motion (Munich)

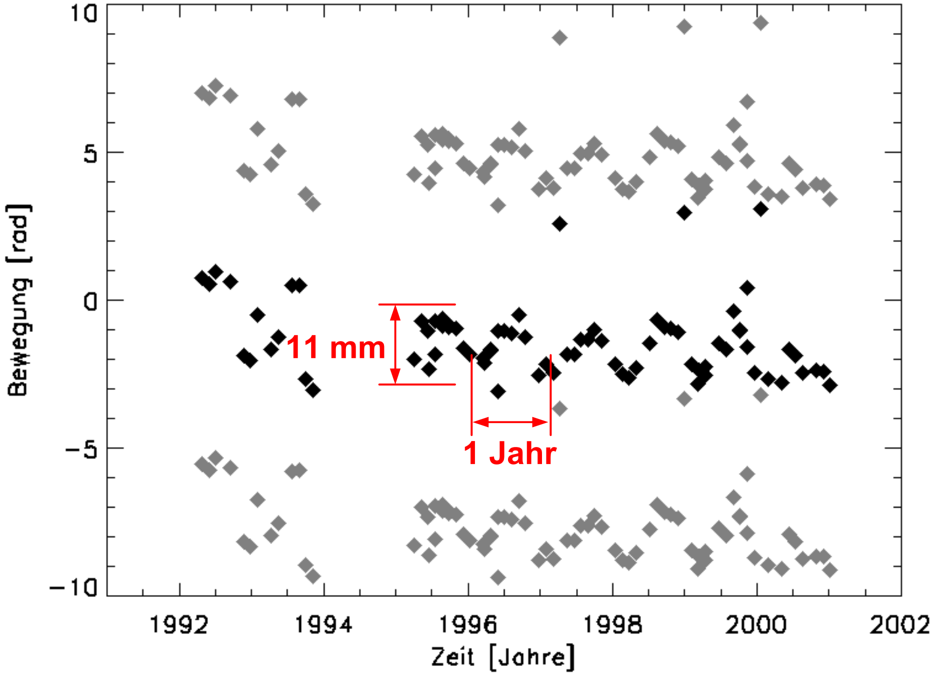

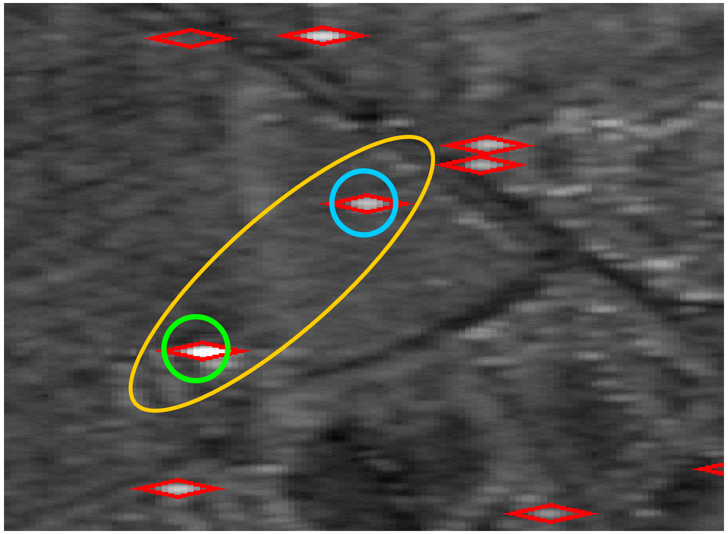

Subsidence in Las Vegas

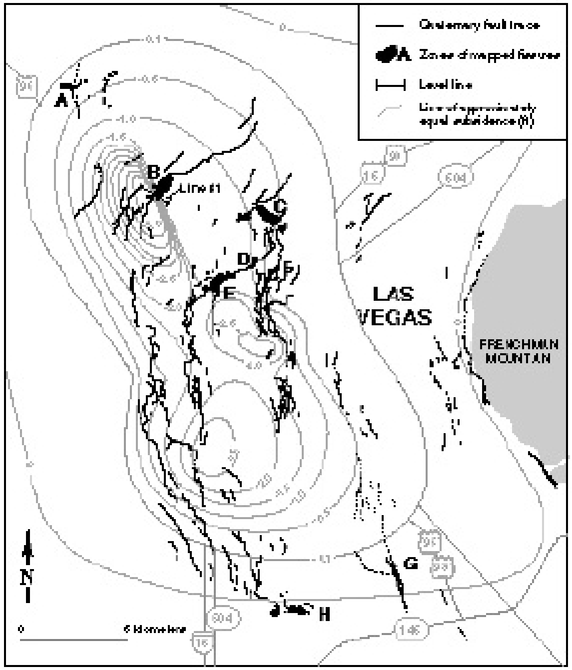

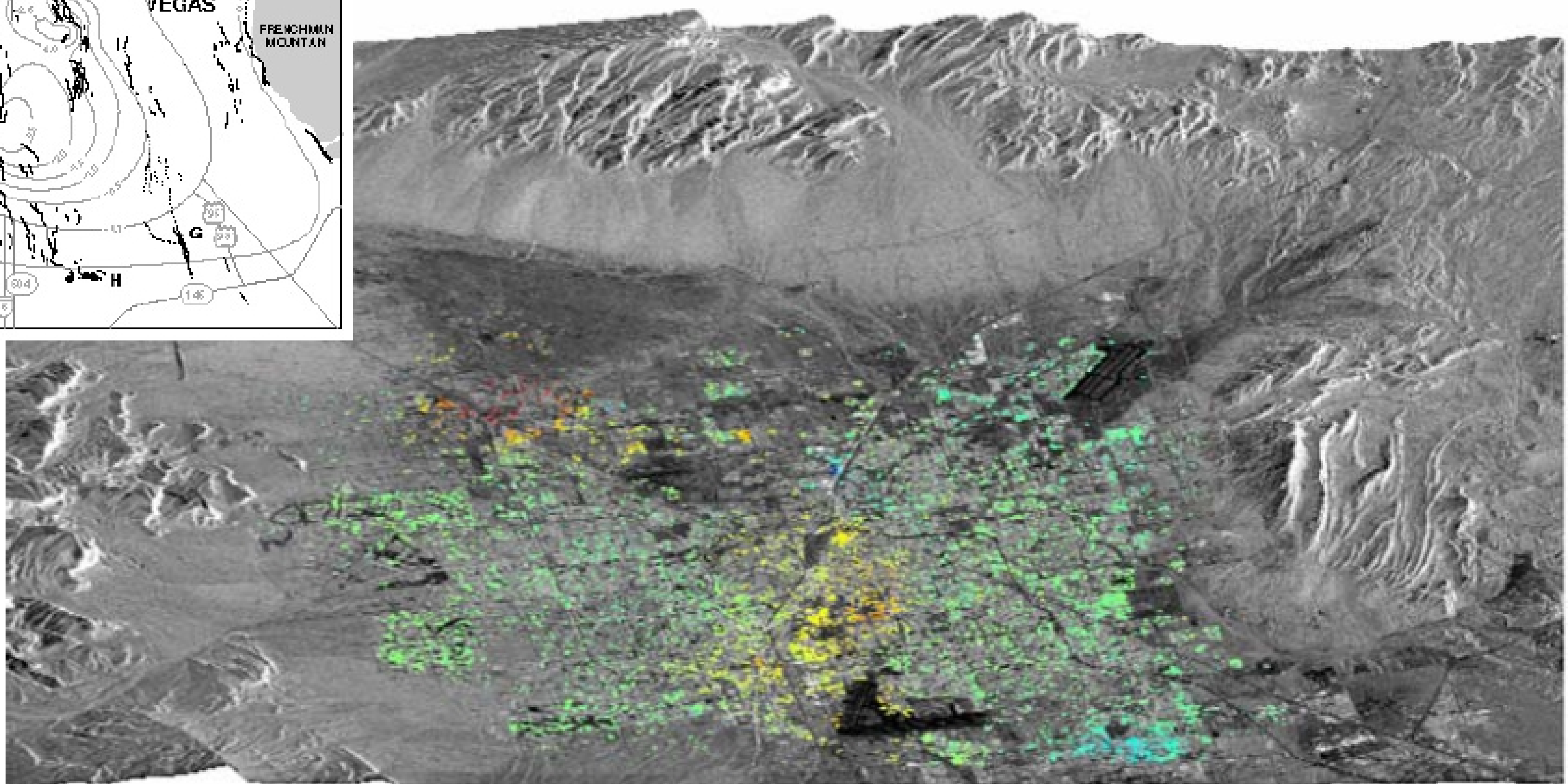

Data © ESA processed by DLR

Subsidence in Las Vegas

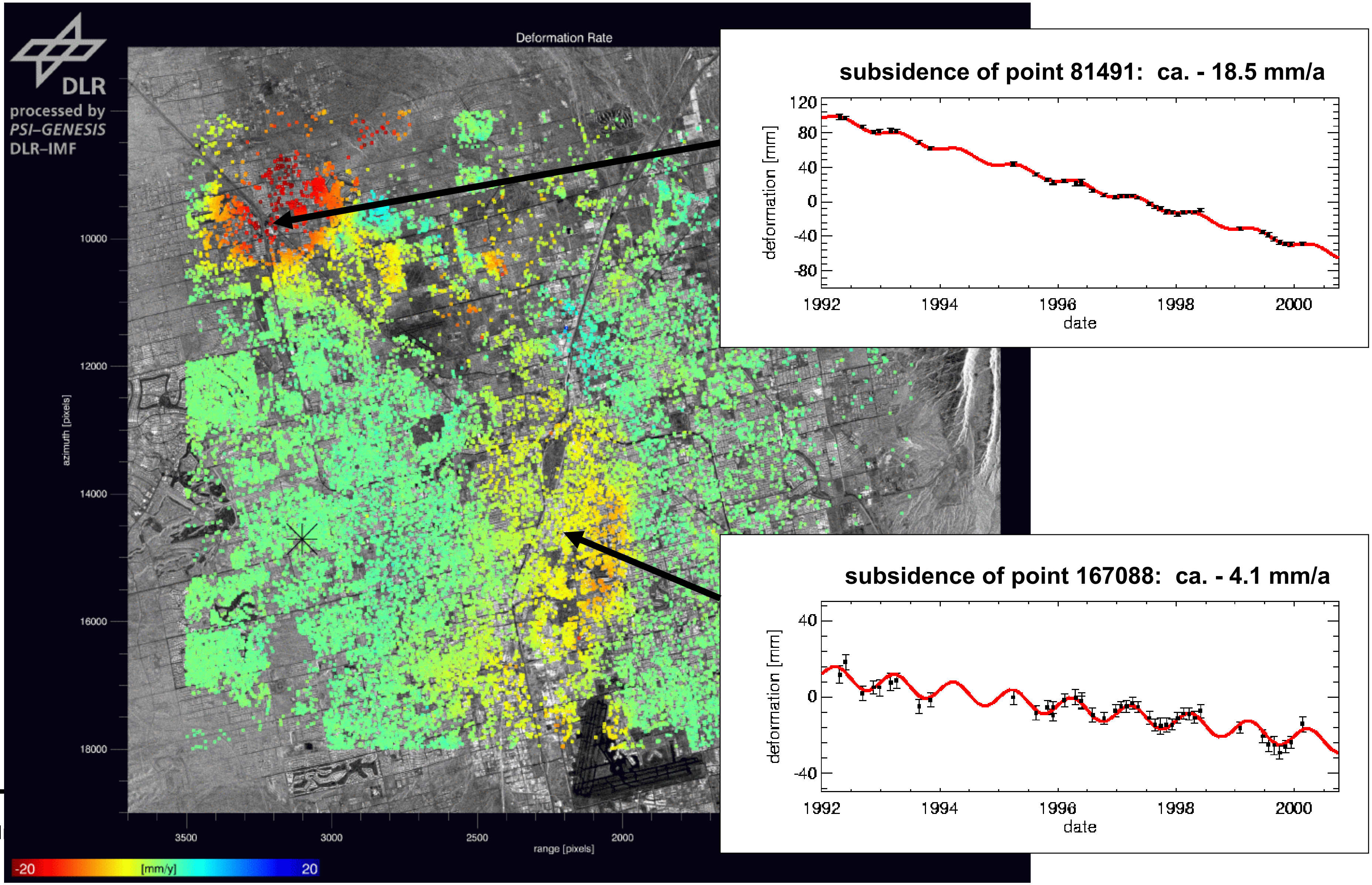

PSI Results Gardanne, France

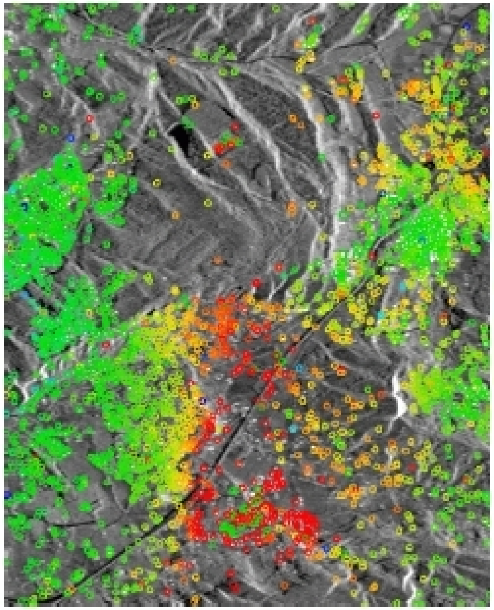

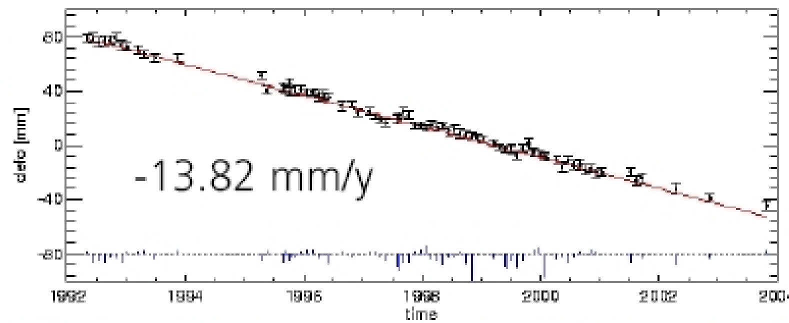

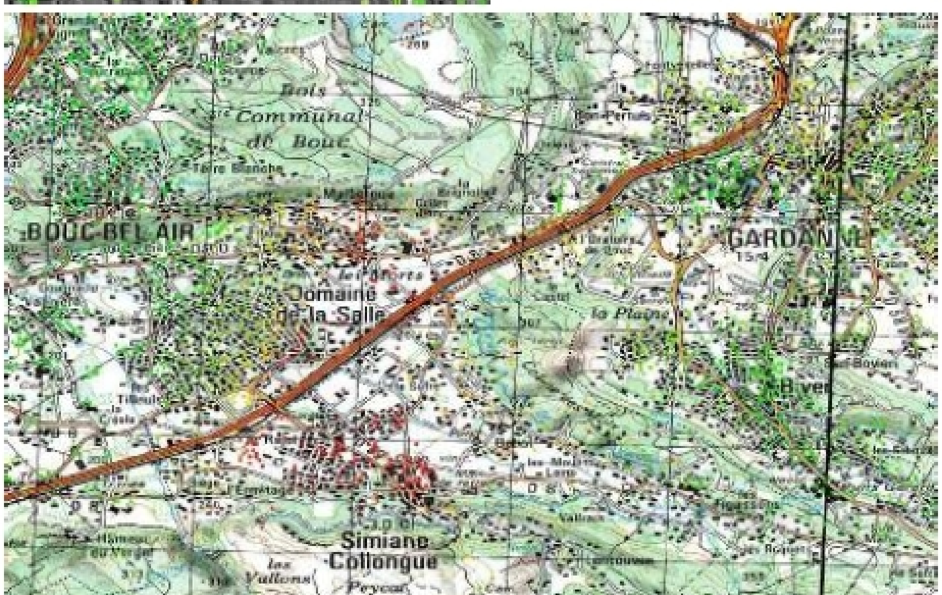

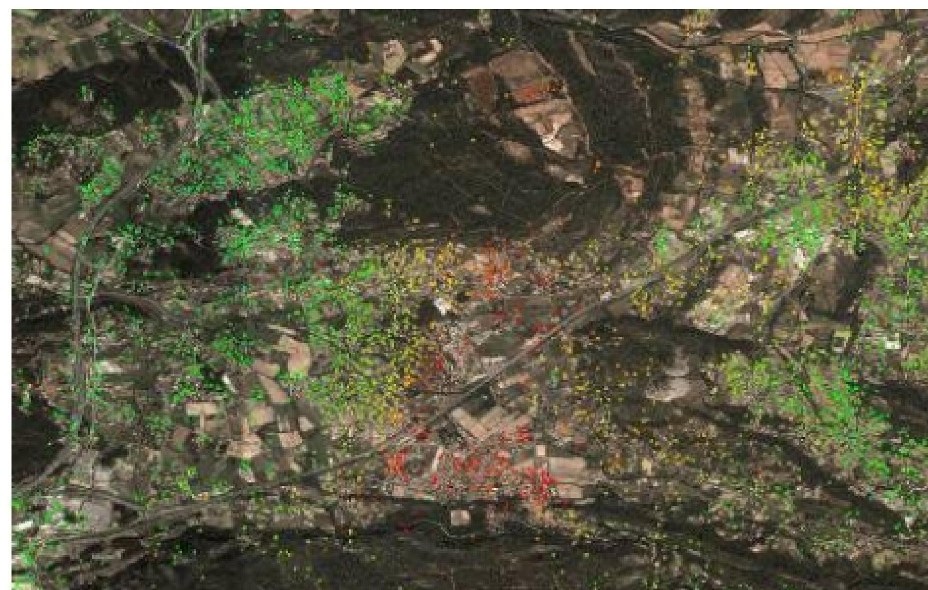

Surface subsidence in London

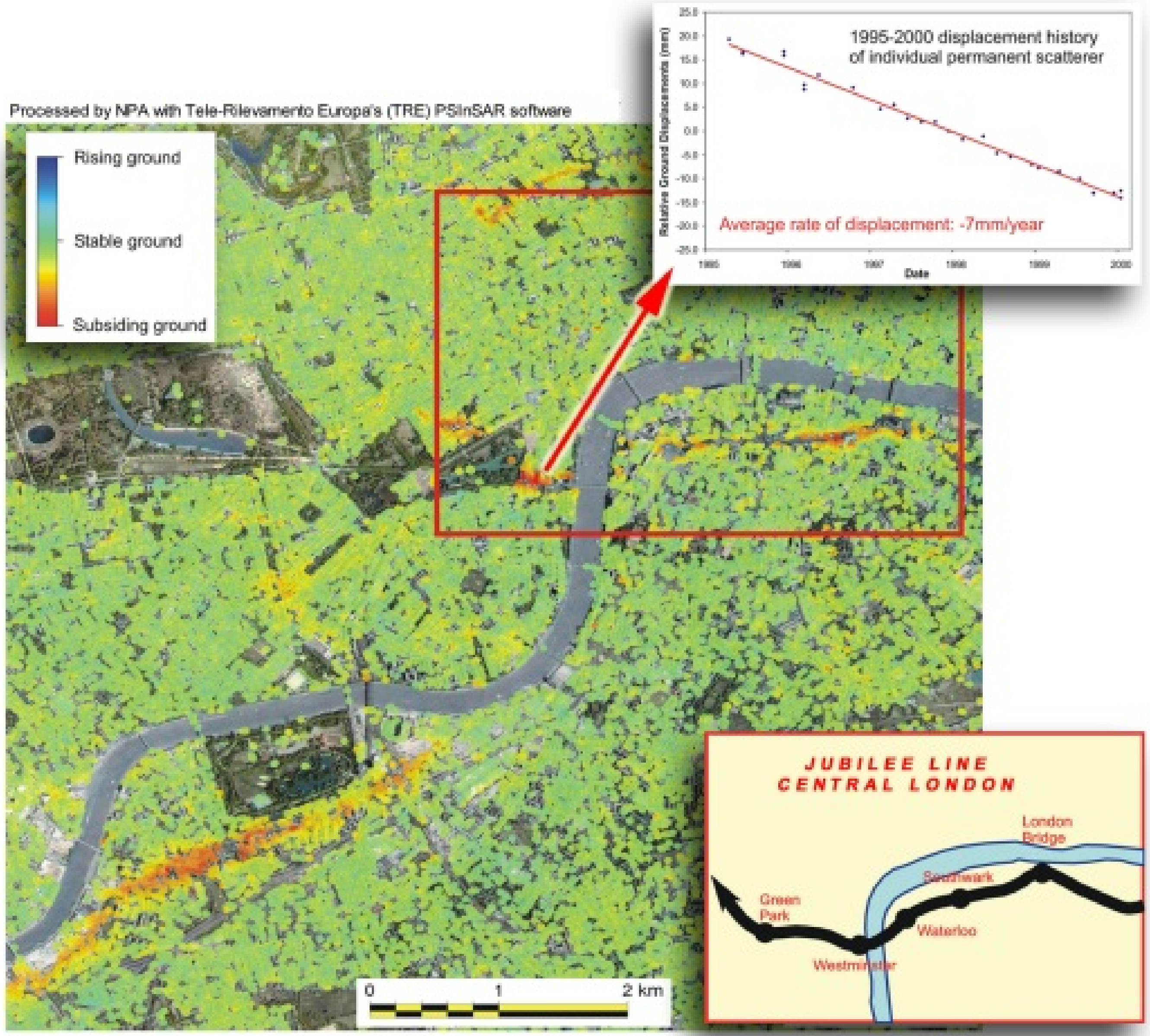

Analysis of Residuals

- Residuals:

$$\phi_{res} = \phi_{atmo} + \phi_{noise}$$

- Atmosphere correlated in space and uncorrelated in time
- Noise is uncorrelated in both space and time
- Separation:
  - Spatial filtering and subsequent interpolation

Atmosphere

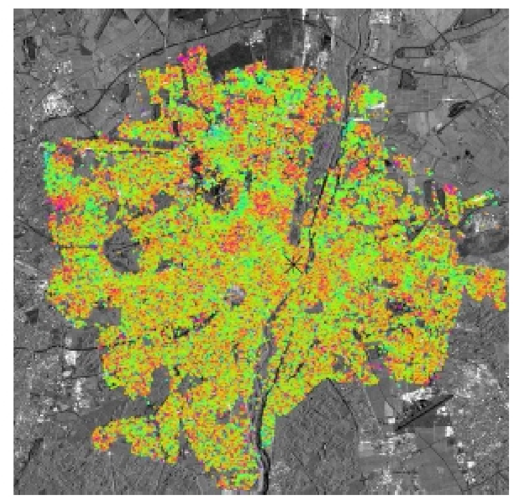

Noise

Derivation of Atmospheric Parameters

- Approximation of Master Atmosphere by temporal averaging and conversion to water vapor content

Atmospheric phase screens for each acquisition

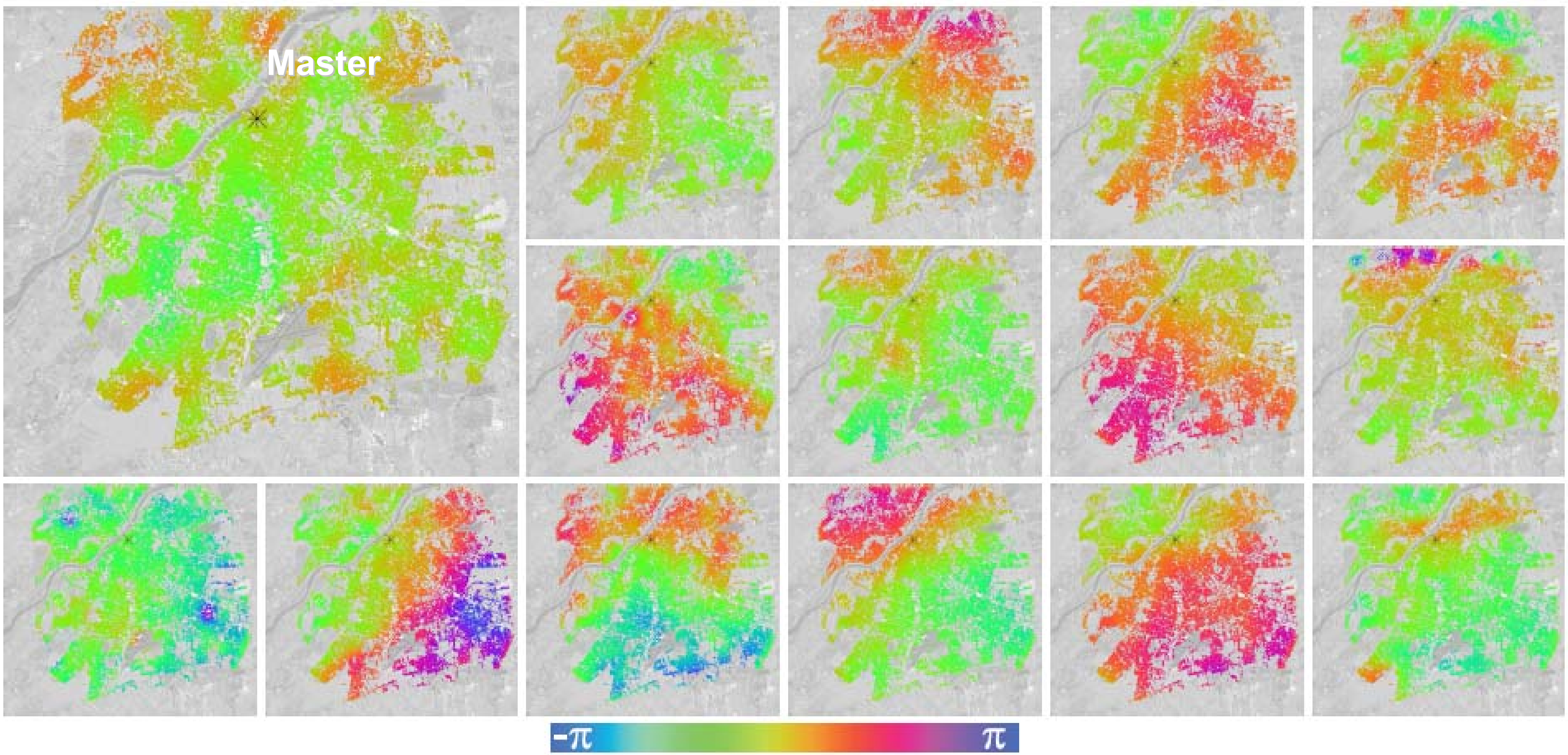

Summary of Results

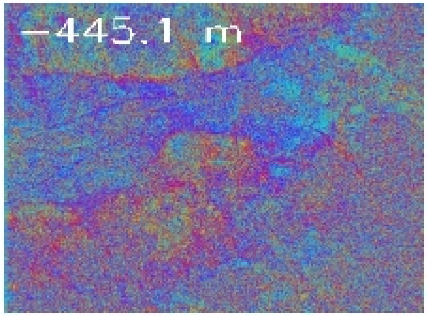

InSAR

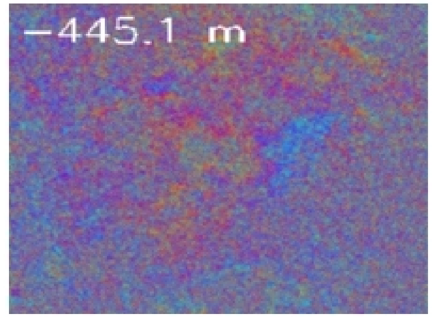

D-InSAR

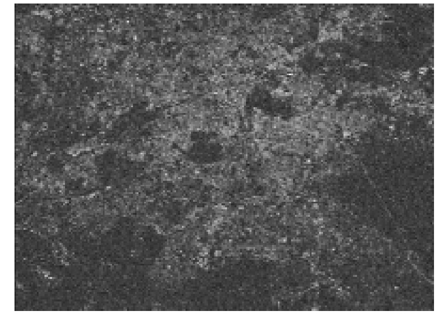

Coherence

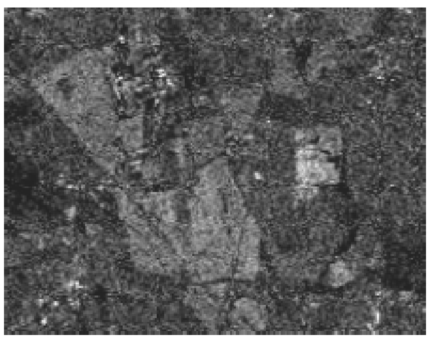

Calibrated Amplitude

multi-look Amplitude

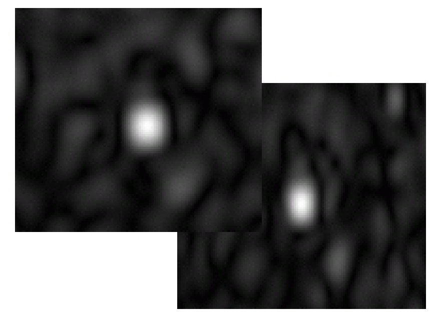

super resolution

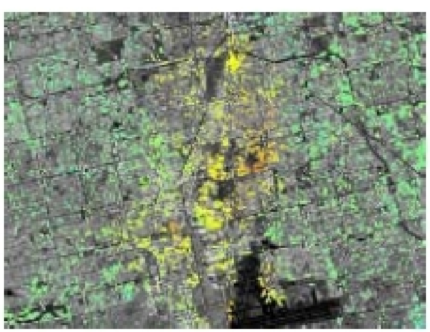

Deformation Map

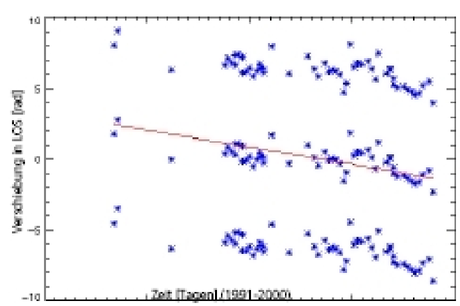

Deformation per PS

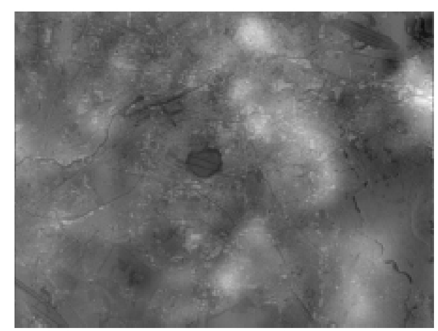

Atmo. Water Vapor